*Atoms* **2015**, *3*, 299-319; doi:10.3390/atoms3030299

OPEN ACCESS

*atoms*

**ISSN 2218-2004**

www.mdpi.com/journal/atoms

*Article*

# Detailed Analysis of Configuration Interaction and Calculation of Radiative Transition Rates in Seven Times Ionized Tungsten (W VIII)

**Jérôme Deprince [1] and Pascal Quinet [1,2,*]**

[1] Astrophysique et Spectroscopie, Université de Mons, Mons B-7000, Belgium; E-Mail: jerome.deprince@gmail.com

[2] IPNAS, Université de Liège, Liège B-4000, Belgium

* Author to whom correspondence should be addressed; E-Mail: Pascal.quinet@umons.ac.be; Tel.: +32-65-373-629.

Academic Editor: Bastiaan J. Braams

*Received: 21 May 2015 / Accepted: 23 June 2015 / Published: 30 June 2015*

**Abstract:** A new set of oscillator strengths and transition probabilities for EUV spectral lines of seven times ionized tungsten (W VIII) is reported in the present paper. These results have been obtained using the pseudo-relativistic Hartree-Fock (HFR) method combined with a semi-empirical optimization of the radial parameters minimizing the discrepancies between computed energy levels and available experimental data. The final physical model considered in the calculations has been chosen further to a detailed investigation of the configuration interaction in this atomic system characterized by complex configurations of the type $4f^{14}5s^25p^5$, $4f^{14}5s^25p^4nl$, $4f^{14}5s5p^6$, $4f^{13}5s^25p^6$, $4f^{13}5s^25p^5nl$ and $4f^{12}5s^25p^6nl$ ($nl$ = 5d, 6s).

**Keywords:** atomic structure; oscillator strengths; transition probabilities; W VIII spectrum

## 1. Introduction

It is now well established that tungsten plays an important role in the development of fusion reactors (see e.g., [1–5]). Indeed, this element has been chosen to be the main component of the divertor of the International Thermonuclear Experimental Reactor (ITER) so that spectral lines of W ions sputtered from the wall to the core plasma provide a key information for plasma emission analysis

and diagnostic purposes. As a consequence, a detailed knowledge of the atomic structure and radiative properties of almost each ionization stage of tungsten is required. Over the past few years, several of our works were focused on the determination of spectroscopic data for neutral to moderately ionized tungsten. More precisely, oscillator strengths and transition probabilities were calculated for a large number of lines in W I [6], W II [7], W III [8], W IV [9], W V [10] and W VI [11]. In all these studies, the pseudo-relativistic Hartree-Fock (HFR) method including a large amount of intravalence and core-valence electronic correlation effects was combined with a semi-empirical process minimizing the discrepancies between calculated and available experimental energy levels. For W I, W II and W III, the accuracy of this approach was assessed through detailed comparisons with experimental radiative lifetimes measured with the time-resolved laser-induced fluorescence (TR-LIF) technique while, for W IV, W V and W VI, our new HFR results were supported by a detailed comparison with transition probabilities obtained using different theoretical methods. In all cases, it was shown that the methodology used for modeling the atomic structure and computing the radiative parameters of lowly ionized tungsten was able to provide reliable spectroscopic data of great interest in fusion research. Let us also mention here that one of our recent papers [12] was dedicated to a critical evaluation of the transition rates available in the literature for electric dipole lines in W I, W II and W III.

The main goal of the present work is to extend all our previous studies related to tungsten ions to the seven times ionized species (W VIII) for which 187 spectral lines were very recently observed leading to the first experimental identification of energy levels in this ion [13]. As we did for the first W ions, we also used here the pseudo-relativistic Hartree-Fock method putting the emphasis on the sensitivity of the radiative rates to electronic correlation effects in this particularly complex atomic system characterized by interacting configurations of the type $4f^{14}5s^25p^5$, $4f^{14}5s^25p^4nl$, $4f^{14}5s5p^6$, $4f^{13}5s^25p^6$, $4f^{13}5s^25p^5nl$ and $4f^{12}5s^25p^6nl$ (*nl* = 5d, 6s). The final theoretical model was then optimized through a semi-empirical adjustment of the radial energy parameters to compute the oscillator strengths and transition probabilities for a set of 227 lines involving experimentally known levels with *gf*-values larger than 0.0001 in the extreme ultraviolet (EUV) wavelength region from 160.9 to 347.0 Å of the W VIII spectrum.

## 2. Available Atomic Data in W VIII

Up until very recently, nearly nothing was known about the atomic structure of seven times ionized tungsten. This lack of knowledge was underlined by Kramida and Shirai [14] who compiled all the classified energy levels and spectral lines of multiply ionized tungsten atoms from $W^{2+}$ to $W^{73+}$. In this compilation, it was reminded that it was by the way uncertain whether the ground state of W VIII was $4f^{13}5s^25p^6\ ^2F°_{7/2}$ or $4f^{14}5s^25p^5\ ^2P°_{3/2}$, making this ion the only known case of p and f orbitals competing for the ground state, as previously noted by Sugar and Kaufman [15]. An isoelectronic study was not even of great help to solve the problem since it was found that the ground configuration was $4f^{11}5s^25p^66s^2$ for the first members of the sequence, Ho I and Er II, $4f^{13}5s^25p^6$ for Hf VI and Ta VII, and $4f^{14}5s^25p^5$ for Re IX and the rest of the sequence. By analyzing the $4f^{13}(^2F°_{7/2})5s^25p^6ns$ and $4f^{14}5s^25p^5(^2P°_{3/2})ns$ series of W VII, Sugar and Kaufman [15] asserted that the ground state of W VIII was probably $4f^{13}5s^25p^6\ ^2F°_{7/2}$, the $4f^{14}5s^25p^5\ ^2P°_{3/2}$ level being predicted 800 ± 700 $cm^{-1}$ above it. This assumption was in agreement with the calculations performed earlier by Carlson *et al.* [16] who

showed that 4f was the least-bound orbital of W VII. Later on, an experimental observation of W VIII spectrum was performed by Veres *et al.* [17] in emission of tokamak plasma but the low spectral resolution did not allow them to identify the observed broad peaks. However, using the weighted average energies of sub-configurations based on the $4f^{13}5s^25p^{6.2}F°_{7/2,5/2}$ and $4f^{14}5s^25p^5\ ^2P°_{3/2,1/2}$ in W VII, taken from [15], Kramida and Shirai [14] predicted the position of the four corresponding energy levels in W VIII at 0 $cm^{-1}$, 17,440 ± 60 $cm^{-1}$, 800 ± 700 $cm^{-1}$ and 87,900 ± 300 $cm^{-1}$, respectively.

Two years ago, the first extensive analysis of the W VIII spectrum was reported by Ryabtsev *et al.* [13] who used two experimental setups installed at the Institute of Spectroscopy in Troitsk (Russia) and at the Observatory of Paris-Meudon (France) for obtaining tungsten ion spectra. In their work, a total of 187 W VIII lines in the region 160–271 Å were identified as transitions from the interacting excited even $4f^{12}5s^25p^65d + 4f^{13}5s^25p^5(5d + 6s) + 4f^{14}5s^25p^4(5d + 6s) + 4f^{14}5s5p^6$ configurations to the low-lying odd configurations $4f^{13}5s^25p^6$ and $4f^{14}5s^25p^5$. This gave rise to the establishment of the energy values of 4 odd- and 98 excited even-parity levels up to 622,123 $cm^{-1}$ with estimated uncertainties ranging from 5 to 18 $cm^{-1}$. It was also firmly established that the ground state of W VIII was $4f^{13}5s^25p^6\ ^2F°_{7/2}$ and the first excited $4f^{14}5s^25p^5\ ^2P°_{3/2}$ level was located 1233 ± 3 $cm^{-1}$ above it, in agreement with the value 800 ± 700 $cm^{-1}$ predicted by Kramida and Shirai [14]. The level identifications reported in [13] were supported by calculations performed using the pseudo-relativistic Hartree-Fock (HFR) method of Cowan [18] combined with a semi-empirical adjustment of the energy parameters. In the HFR model considered by these latter authors, also used for providing transition probabilities corresponding to the experimentally observed spectral lines, the $4f^{13}5s^25p^6$ and $4f^{14}5s^25p^5$ odd-parity configurations and the $4f^{12}5s^25p^6(5d + 6s + 6d)$, $4f^{13}5s^25p^5(5d + 6s + 6d + 7s)$, $4f^{14}5s^25p^4(5d + 6s + 6d + 7s)$, $4f^{14}5s5p^6$ and $4f^{14}5s5p^55f$ even-parity configurations were included. Furthermore, these calculations revealed a very strong mixing in the eigenvector compositions for many excited even-parity states, neither the *LS*-coupling nor the *jj*-coupling appearing to give a good overall description of the energy levels.

## 3. Configuration Interaction Analysis

As mentioned in the previous section, the only available radiative rates in W VIII were reported by Ryabtsev *et al.* [13] who used the HFR method with a rather unbalanced physical model since it included only 2 odd-parity configurations ($4f^{13}5s^25p^6$ and $4f^{14}5s^25p^5$) for 13 configurations ($4f^{12}5s^25p^6(5d + 6s + 6d)$, $4f^{13}5s^25p^5(5d + 6s + 6d + 7s)$, $4f^{14}5s^25p^4(5d + 6s + 6d + 7s)$, $4f^{14}5s5p^6$ and $4f^{14}5s5p^55f$) in the even parity. In order to estimate the effects of configuration interaction on the radiative parameters of W VIII, different physical models based on the pseudo-relativistic Hartree-Fock method were considered in the present work. In all of them, the electrostatic interaction Slater integrals, $F^k$, $G^k$ and $R^k$ were scaled down by a factor 0.85, as suggested by Cowan [18] while the spin-orbit parameters were kept to their *ab initio* values. The first model used, HFR(A), was the same as the one considered in [13] for computing their transition probabilities. The second model, HFR(B), was built to rebalance configuration interaction within both parities by adding to the HFR(A) model the $4f^{12}5s^25p^6(5f + 6p) + 4f^{13}5s^25p^5(5f + 6p) + 4f^{14}5s^25p^4(5f + 6p) + 4f^{14}5s5p^5(5d + 6s + 6d + 7s)$ odd-parity configurations, leading to 12 and 13 configurations in each parity, respectively. In the third model, HFR(C), we proceeded in a more systematic way since all the configurations of the type $(4f + 5s + 5p)^k nl$ ($k$ = 20 or 21, $nl$ = 5d, 5f, 6s, 6p, 6d, 7s) with one or two holes in the 4f, 5s and 5p subshells were included in the multiconfiguration

expansions. This gave rise to the 18 odd-parity configurations $4f^{13}5s^25p^6$, $4f^{14}5s^25p^5$, $4f^{14}5s^25p^4(5f + 6p)$, $4f^{14}5s5p^5(5d + 6s + 6d + 7s)$, $4f^{13}5s^25p^5(5f + 6p)$, $4f^{13}5s5p^6(5d + 6s + 6d + 7s)$, $4f^{14}5p^6(5f + 6p)$, $4f^{12}5s^25p^6(5f + 6p)$ and the 21 even-parity configurations $4f^{14}5s5p^6$, $4f^{14}5s^25p^4(5d + 6s + 6d + 7s)$, $4f^{14}5s5p^5(5f + 6p)$, $4f^{13}5s^25p^5(5d + 6s + 6d + 7s)$, $4f^{13}5s5p^6(5f + 6p)$, $4f^{14}5p^6(5d + 6s + 6d + 7s)$, $4f^{12}5s^25p^6(5d + 6s + 6d + 7s)$. Finally, a fourth model, HFR(D), was tested. In this one, the same set of interacting configurations as the one considered in model HFR(C) was included with the additional permission that one electron could be excited on the 6f or the 7p subshell, giving rise to a total of 26 odd-parity and 25 even-parity configurations. Using the four HFR models presented hereabove, we computed and compared the radiative lifetimes for the 250 lowest even-parity energy levels with τ-values smaller than 100 ns. These comparisons are summarized in Figure 1 showing the ratios τ(B)/τ(A), τ(C)/τ(B) and τ(D)/τ(C), respectively. When looking at Figure 1a, it is clear that the numerous missing odd-parity configurations in the HFR(A) model, similar to the one used by Ryabtsev *et al.* [13], make without doubt this latter model insufficient to provide a reliable set of transition probabilities, the mean deviation between the HFR(B) and HFR(A) lifetimes being found to be within about 30%, with notable discrepancies reaching a factor of 2–3 in some cases. Moreover, Figure 1b shows that the HFR(B) model does not either include enough configuration interaction to give a reasonable accuracy of the radiative lifetime calculations, the differences between the data computed with models HFR(C) and HFR(B) still reaching a factor of 1.5–2 in many cases. However, as shown in Figure 1c, the excitations of one electron to the 6f or 7p subshell included in model HFR(D) do not really change the results obtained in model HFR(C), the mean deviation between both sets of lifetimes not exceeding 2%. We can therefore conclude that the one single excitation from 4f, 5s and 5p to *nl* orbitals with *nl* = 5d, 5f, 6s, 6p, 6d and 7s, as considered in the configuration interaction expansions of model HFR(C), should form a good basis for computing the spectroscopic data in W VIII.

Furthermore, it is also interesting to estimate the influence of the double excitations on the radiative parameters. Indeed, for transitions of the type $4f^{14}5s^25p^5 – 4f^{14}5s^25p^45d$ and $4f^{13}5s^25p^6 – 4f^{13}5s^25p^55d$, the $5p^2 \rightarrow 5d^2$ double excitation in the lower odd-parity state leads to an allowed transition to the upper even-parity state with an electric dipole matrix element which is equal in magnitude to that for the primary transition. In order to evaluate this effect on the decay rates, we extended the multiconfiguration expansion of model HFR(C) with the two additional odd-parity configurations $4f^{14}5s^25p^35d^2$ and $4f^{13}5s^25p^45d^2$, giving rise to model HFR(E). Finally, as similar speculations can be made for the double excitation $4f^2 \rightarrow 5d^2$ in the case of the $4f^{14}5s^25p^5 – 4f^{13}5s^25p^55d$ and $4f^{13}5s^25p^6 – 4f^{12}5s^25p^65d$ transitions and for the double excitation $5p^2 \rightarrow 6s^2$ in the case of the $4f^{14}5s^25p^5 – 4f^{14}5s^25p^46s$ and $4f^{13}5s^25p^6 – 4f^{13}5s^25p^56s$ transitions, the odd-parity configurations $4f^{12}5s^25p^55d^2$ and $4f^{11}5s^25p^65d^2$ were added to model HFR(E) to give model HFR(F), while $4f^{14}5s^25p^36s^2$ and $4f^{13}5s^25p^46s^2$ were added to model HFR(F) to give model HFR(G). The radiative lifetimes calculated with these latter models are compared to those obtained with HFR(C) in Figure 2. As observed in this figure, if the $5p^2 \rightarrow 6s^2$, considered in model HFR(G) do not change the final results (see Figure 2c), it is not the same for the $5p^2 \rightarrow 5d^2$ and $4f^2 \rightarrow 5d^2$ excitations, respectively included in models HFR(E) and HFR(F), which both lead to non negligible changes in the computed radiative lifetimes by about 20% (see Figures 2a,2b). This is nevertheless not very surprising since this kind of effect was already highlighted by Quinet and Hansen [19] who

pointed out the influence of $3p^2 \rightarrow 3d^2$ core excitation on the $3p^6 3d^N - 3p^5 3d^{N+1}$ transition rates in iron group elements.

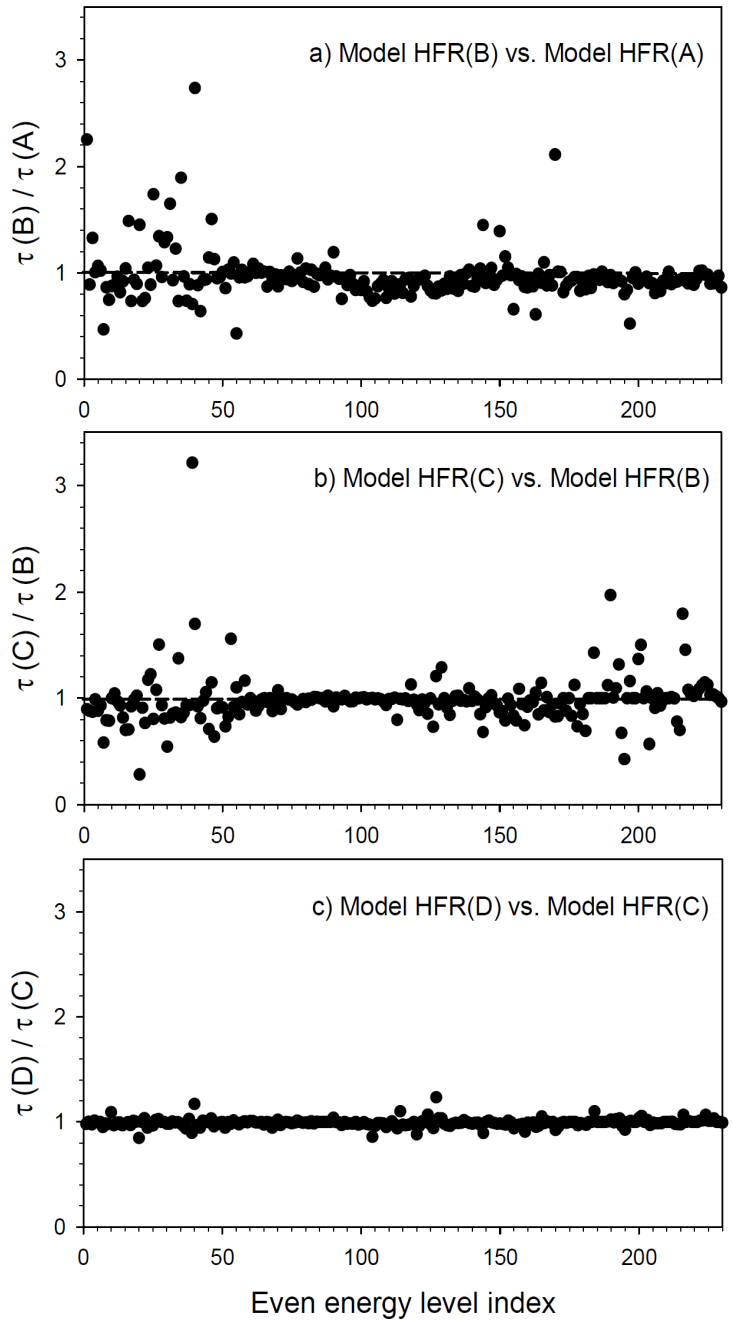


**Figure 1.** Comparison between radiative lifetimes obtained in the present work using different HFR models for short-lived even-parity energy levels ($\tau < 100$ ns) in W VIII. In each panel, the y-axis gives the ratio of $\tau$ -values computed with two successive models including only single excitations (see text) while the x-axis corresponds to the level indexes, assigned according to the order of increasing energies.

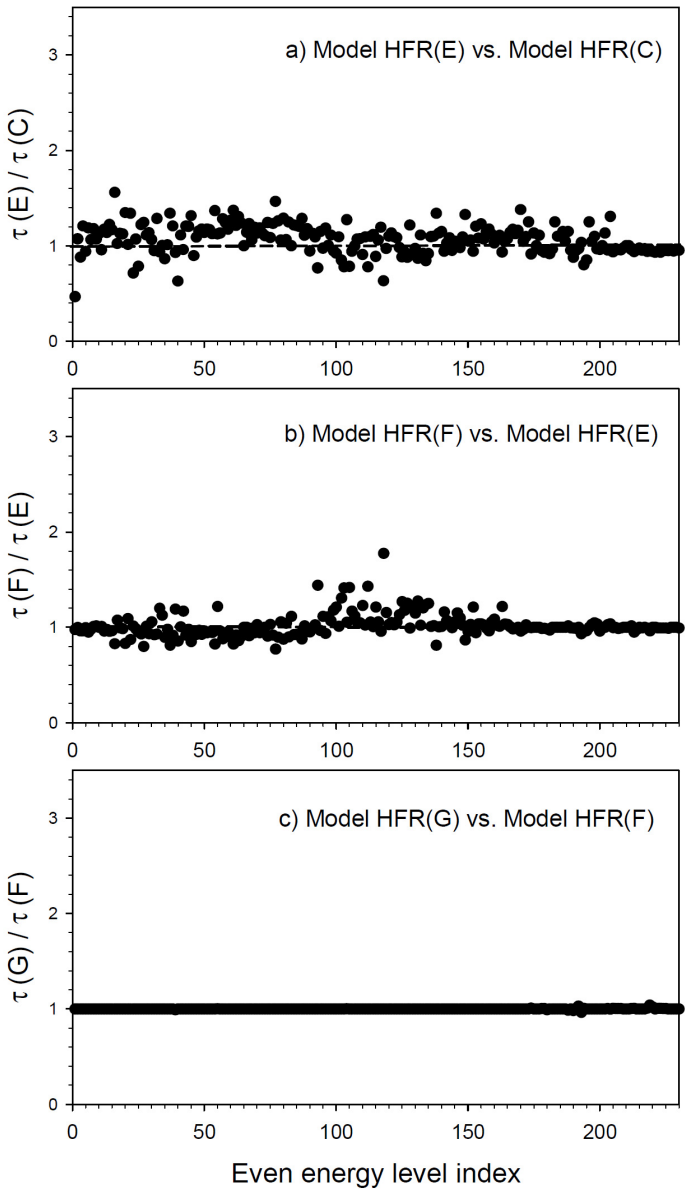


**Figure 2.** Comparison between radiative lifetimes obtained in the present work using different HFR models for short-lived even-parity energy levels ($\tau$ < 100 ns) in W VIII. In each panel, the y-axis gives the ratio of $\tau$-values computed with two successive models including both single and double excitations (see text) while the x-axis corresponds to the level indexes, assigned according to the order of increasing energies.

## 4. Radiative Parameter Calculations

Further to the detailed discussion presented in the previous section, HFR(F) was chosen as the final model to compute the radiative parameters in W VIII. To summarize, the following configurations were explicitly included in the calculations: $4f^{13}5s^25p^6 + 4f^{14}5s^25p^5 + 4f^{14}5s^25p^4(5f + 6p) + 4f^{14}5s5p^5(5d + 6s + 6d + 7s) + 4f^{13}5s^25p^5(5f + 6p) + 4f^{13}5s5p^6(5d + 6s + 6d + 7s) + 4f^{14}5p^6(5f + 6p) + 4f^{12}5s^25p^6(5f + 6p) + 4f^{14}5s^25p^35d^2 + 4f^{13}5s^25p^45d^2 + 4f^{12}5s^25p^55d^2 + 4f^{11}5s^25p^65d^2$ (odd parity) and $4f^{14}5s5p^6 + 4f^{14}5s^25p^4(5d + 6s + 6d + 7s) + 4f^{14}5s5p^5(5f + 6p) + 4f^{13}5s^25p^5(5d + 6s + 6d + 7s) + 4f^{13}5s5p^6(5f + 6p) + 4f^{14}5p^6(5d + 6s + 6d + 7s) + 4f^{12}5s^25p^6(5d + 6s + 6d + 7s)$ (even parity). This

model was then combined with a semi-empirical adjustment of the radial energy parameters in order to minimize the discrepancies between calculated and available experimental energy levels. The strategy followed in the fitting process was exactly the same as the one developed by Ryabtsev *et al.* [13] to the extent that, starting with the numerical values given in their paper, the same parameters were adjusted with the same constraints as those used by these latter authors. This allowed us simply to adapt and optimize the final radial parameters to our physical model including a much larger number of interacting configurations than the model used in [13].

The numerical values of the radial parameters adopted in our work are reported in Table 1 while the calculated energy levels are compared to the experimental data in Table 2. For the 98 even-parity levels, the standard deviation of the fit was found to be equal to 438 $cm^{-1}$ which is comparable to the value of 443 $cm^{-1}$ obtained by Ryabtsev *et al.* [13]. When looking at the table, it appears that the ordering of experimental and calculated energy levels can be different in a few cases. This is simply due to the fact that some experimental level values are close to each other, with a difference of the same order of magnitude as the standard deviation mentioned above. However, in any case, the ordering of the calculated energies always corresponds to the observed one within a *J*-matrix. Table 2 also lists the first three *LS*-components for each level. We can note that, as expected, most of the even-parity states are very strongly mixed and, as already pointed out by Ryabtsev *et al.*, the *jj*-coupling scheme given by these authors appears a bit more appropriate than the *LS* one, with average eigenvector purities of 45% and 32%, respectively. It is also worth mentioning that, if *LS* purities of 100% were reported by Ryabtsev *et al.*, for the four levels belonging to the $4f^{13}5s^25p^6$ and $4f^{14}5s^25p^5$ odd-parity configurations, it is no more the case in our extended configuration interaction model which gives slightly reduced purities of 97%–98% for those levels. In spite of their very strong mixing, the first *LS*-component of each level is given in boldface in Table 2.

**Table 1.** Numerical values (in $cm^{-1}$) of the radial energy parameters adopted in the Hartree-Fock (HFR) calculations.

| Configuration | Parameter | Fit | Unc. | Note [a] | Fit/HFR |
|---|---|---|---|---|---|
| Odd parity | | | | | |
| $4f^{13}5s^25p^6$ | $E_{av}$ | 29,053 | 0 | | |
| | ζ (4f) | 4971 | 0 | | 0.988 |
| $4f^{14}5s^25p^5$ | $E_{av}$ | 51,968 | 0 | | |
| | ζ(5p) | 59,148 | 0 | | 1.003 |
| Even parity | | | | | |
| $4f^{14}5s5p^6$ | $E_{av}$ | 377,512 | | f | |
| $4f^{13}5s^25p^55d$ | $E_{av}$ | 403,242 | 249 | | |
| | ζ (4f) | 5022 | 48 | r11 | 0.995 |
| | ζ(5p) | 60,705 | 127 | r2 | 0.984 |
| | ζ(5d) | 4716 | 109 | r10 | 0.988 |
| | $F^2$(4f,5p) | 52,909 | 1606 | r12 | 0.785 |
| | $F^2$(4f,5d) | 35,345 | 2124 | r4 | 0.780 |
| | $F^4$(4f,5d) | 17,165 | 1031 | r4 | 0.780 |
| | $F^2$(5p,5d) | 63,984 | 2700 | r7 | 0.815 |

**Table 1.** *Cont.*

| Configuration | Parameter | Fit | Unc. | Note [a] | Fit/HFR |
|---|---|---|---|---|---|
| | $G^2(4f,5p)$ | 28,161 | 1313 | r3 | 1.025 |
| | $G^4(4f,5p)$ | 23,435 | 1092 | r3 | 1.025 |
| | $G^1(4f,5d)$ | 13,991 | 413 | r5 | 0.876 |
| | $G^3(4f,5d)$ | 13,111 | 387 | r5 | 0.876 |
| | $G^5(4f,5d)$ | 10,482 | 309 | r5 | 0.876 |
| | $G^1(5p,5d)$ | 67,786 | 607 | r1 | 0.711 |
| | $G^3(5p,5d)$ | 42,728 | 383 | r1 | 0.711 |
| $4f^{13}5s^25p^56d$ | $E_{av}$ | 775,400 | | f | |
| $4f^{13}5s^25p^56s$ | $E_{av}$ | 542,642 | 139 | | |
| | $\zeta(4f)$ | 5033 | 48 | r11 | 0.995 |
| | $\zeta(5p)$ | 61,895 | 130 | r2 | 0.984 |
| | $F^2(4f,5p)$ | 53,429 | 1622 | r12 | 0.785 |
| | $G^2(4f,5p)$ | 28,352 | 1322 | r3 | 1.025 |
| | $G^4(4f,5p)$ | 23,664 | 1103 | r3 | 1.025 |
| | $G^3(4f,6s)$ | 6873 | 2032 | | 1.294 |
| | $G^1(5p,6s)$ | 9385 | 742 | r13 | 0.881 |
| $4f^{13}5s^25p^57s$ | $E_{av}$ | 813,134 | | f | |
| $4f^{14}5s^25p^45d$ | $E_{av}$ | 420,745 | 400 | | |
| | $F^2(5p,5p)$ | 77,035 | 2775 | r14 | 0.834 |
| | $\zeta(5p)$ | 58,775 | 123 | r2 | 0.984 |
| | $\zeta(5d)$ | 4465 | 103 | r10 | 0.988 |
| | $F^2(5p,5d)$ | 62,865 | 2653 | r7 | 0.815 |
| | $G^1(5p,5d)$ | 66,467 | 595 | r1 | 0.711 |
| | $G^3(5p,5d)$ | 41,892 | 375 | r1 | 0.711 |
| $4f^{14}5s^25p^46d$ | $E_{av}$ | 778,313 | | f | |
| $4f^{14}5s^25p^46s$ | $E_{av}$ | 550,299 | 268 | | |
| | $F^2(5p,5p)$ | 77,932 | 2807 | r14 | 0.838 |
| | $\zeta(5p)$ | 59,932 | 126 | r2 | 0.984 |
| | $G^1(5p,6s)$ | 9397 | 743 | r13 | 0.881 |
| $4f^{14}5s^25p^47s$ | $E_{av}$ | 813,793 | | f | |
| $4f^{14}5s5p^56p$ | $E_{av}$ | 992,590 | | f | |
| $4f^{14}5s5p^55f$ | $E_{av}$ | 1092,223 | | f | |
| $4f^{12}5s^25p^65d$ | $E_{av}$ | 429,283 | 138 | | |
| | $F^2(4f,4f)$ | 149,065 | 2553 | | 0.843 |
| | $F^4(4f,4f)$ | 111,500 | 6763 | | 0.991 |
| | $F^6(4f,4f)$ | 77,044 | 3283 | | 0.947 |
| | $\alpha$ | 22 | | f | |
| | $\beta$ | −1000 | | f | |
| | $\gamma$ | −70 | | f | |
| | $\zeta(4f)$ | 5200 | 49 | r11 | 0.995 |
| | $\zeta(5d)$ | 4977 | 115 | r10 | 0.988 |
| | $F^2(4f,5d)$ | 36,300 | 1467 | r6 | 0.785 |
| | $F^4(4f,5d)$ | 17,592 | 711 | r6 | 0.785 |

**Table 1.** *Cont.*

| Configuration | Parameter | Fit | Unc. | Note [a] | Fit/HFR |
|---|---|---|---|---|---|
| | $G^1(4f,5d)$ | 13,832 | 408 | r5 | 0.876 |
| | $G^3(4f,5d)$ | 13,147 | 388 | r5 | 0.876 |
| | $G^5(4f,5d)$ | 10,564 | 312 | r5 | 0.876 |
| $4f^{12}5s^25p^66d$ | $E_{av}$ | 819,431 | | f | |
| $4f^{12}5s^25p^66s$ | $E_{av}$ | 579,803 | | f | |
| | $F^2(4f,4f)$ | 147,636 | | f | 0.833 |
| | $F^4(4f,4f)$ | 110,752 | | f | 0.982 |
| | $F^6(4f,4f)$ | 78,585 | | f | 0.963 |
| | $\alpha$ | 22 | | f | |
| | $\beta$ | −1000 | | f | |
| | $\gamma$ | −70 | | f | |
| | $\zeta(4f)$ | 5161 | | f | 0.985 |
| | $G^3(4f,6s)$ | 3974 | | f | 0.758 |
| $4f^{13}5s^25p^55d$ – $4f^{14}5s^25p^45d$ | $D^2(4f,5p;4f,4f)$ | −5660 | 51 | r8 | 0.864 |
| | $D^4(4f,5p;4f,4f)$ | −309 | 3 | r8 | 0.864 |
| | $D^2(5p,5p;4f,5p)$ | −34,864 | 312 | r8 | 0.864 |
| | $D^2(5p,5d;4f,5d)$ | −27,246 | 244 | r8 | 0.864 |
| | $D^4(5p,5d;4f,5d)$ | −17,855 | 160 | r8 | 0.864 |
| | $E^1(5p,5d;4f,5d)$ | −24,107 | 216 | r8 | 0.864 |
| | $E^3(5p,5d;4f,5d)$ | −18,067 | 162 | r8 | 0.864 |
| $4f^{13}5s^25p^55d$ – $4f^{12}5s^25p^65d$ | $D^2(4f,4f;4f,5p)$ | −3792 | 8 | r9 | 0.827 |
| | $D^4(4f,4f;4f,5p)$ | 858 | 2 | r9 | 0.827 |
| | $D^2(4f,5p;5p,5p)$ | −32,556 | 68 | r9 | 0.827 |
| | $D^2(4f,5d;5p,5d)$ | −25,604 | 54 | r9 | 0.827 |
| | $D^4(4f,5d;5p,5d)$ | −16,845 | 35 | r9 | 0.827 |
| | $E^1(4f,5d;5p,5d)$ | −22,393 | 47 | r9 | 0.827 |
| | $E^3(4f,5d;5p,5d)$ | −16,982 | 36 | r9 | 0.827 |
| $4f^{14}5s^25p^45d$ – $4f^{12}5s^25p^65d$ | $D^2(4f,4f;5p,5p)$ | 24,592 | 52 | r9 | 0.827 |
| | $D^4(4f,4f;5p,5p)$ | 20,291 | 43 | r9 | 0.827 |
| $4f^{13}5s^25p^56s$ – $4f^{14}5s^25p^46s$ | $D^2(4f,5p,4f,4f)$ | −6391 | | f | 1.000 |
| | $D^4(4f,5p;4f,4f)$ | −244 | | f | 1.000 |
| | $D^2(5p,5p;4f,5p)$ | −40,487 | | f | 1.000 |

[a] f: fixed parameter from [13]; r n : parameters linked by their corresponding HFR ratios.

**Table 2.** Comparison between the energy levels computed in the present work and the experimentally known values available in seven times ionized tungsten (W VIII). Energies are given in $cm^{-1}$.

| Index | $E_{exp}$ [a] | $E_{calc}$ [b] | ΔE [c] | J | Percentage Composition in LS-Coupling [d] |
|---|---|---|---|---|---|
| | | | | | Odd Parity |
| 1° | 0 | 0 | 0 | 7/2 | 98 **$4f^{13}5p^6$ $^2$F** |
| 2° | 1233 | 1233 | 0 | 3/2 | 98 **$4f^{14}5p^5$ $^2$P** |
| 3° | 17,410 | 17,410 | 0 | 5/2 | 98 **$4f^{13}5p^6$ $^2$F** |
| 4° | 89,123 | 89,123 | 0 | 1/2 | 97 **$4f^{14}5p^5$ $^2$P** |
| | | | | | Even Parity |
| 1 | 377,119 | 377,140 | −21 | 9/2 | 28 **$4f^{13}5p^5(^3F)5d$ $^2$H** + 23 $4f^{13}5p^5(^1D)5d$ $^2$G + 8 $4f^{13}5p^5(^3F)5d$ $^2$G |
| 2 | 377,288 | 376,992 | 296 | 3/2 | 25 **$4f^{13}5p^5(^1D)5d$ $^2$P** + 18 $4f^{13}5p^5(^3D)5d$ $^4$F + 15 $4f^{13}5p^5(^3D)5d$ $^4$P |
| 3 | 377,867 | 377,714 | 153 | 5/2 | 21 **$4f^{13}5p^5(^3D)5d$ $^4$F** + 12 $4f^{14}5p^4(^1S)5d$ $^2$D + 9 $4f^{13}5p^5(^3F)5d$ $^2$F |
| 4 | 380,899 | 381,127 | −228 | 9/2 | 18 **$4f^{13}5p^5(^1G)5d$ $^2$G** + 18 $4f^{13}5p^5(^3G)5d$ $^2$G + 14 $4f^{13}5p^5(^3F)5d$ $^2$G |
| 5 | 382,019 | 382,285 | −266 | 7/2 | 22 **$4f^{13}5p^5(^1D)5d$ $^2$F** + 15 $4f^{13}5p^5(^3D)5d$ $^2$G + 13 $4f^{13}5p^5(^3F)5d$ $^2$F |
| 6 | 383,133 | 383,535 | −402 | 5/2 | 18 **$4f^{13}5p^5(^3D)5d$ $^2$F** + 17 $4f^{13}5p^5(^1D)5d$ $^2$D + 10 $4f^{14}5p^4(^1S)5d$ $^2$D |
| 7 | 384,400 | 383,622 | 778 | 9/2 | 24 **$4f^{13}5p^5(^1G)5d$ $^2$H** + 20 $4f^{13}5p^5(^3G)5d$ $^4$H + 11 $4f^{13}5p^5(^3D)5d$ $^4$G |
| 8 | 386,704 | 386,497 | 207 | 5/2 | 16 **$4f^{13}5p^5(^3F)5d$ $^2$D** + 11 $4f^{13}5p^5(^3G)5d$ $^4$D + 9 $4f^{13}5p^5(^3F)5d$ $^4$P |
| 9 | 391,541 | 392,282 | −741 | 9/2 | 14 **$4f^{13}5p^5(^1D)5d$ $^2$G** + 13 $4f^{12}5p^6(^3H)5d$ $^2$G + 5 $4f^{13}5p^5(^3G)5d$ $^2$H |
| 10 | 393,992 | 393,539 | 453 | 7/2 | 18 **$4f^{12}5p^6(^3H)5d$ $^2$F** + 14 $4f^{13}5p^5(^3G)5d$ $^2$F |
| 11 | 395,276 | 395,201 | 75 | 5/2 | 19 **$4f^{13}5p^5(^3D)5d$ $^2$F** + 17 $4f^{13}5p^5(^3D)5d$ $^4$D + 16 $4f^{13}5p^5(^3D)5d$ $^4$F |
| 12 | 395,471 | 395,624 | −153 | 7/2 | 14 **$4f^{12}5p^6(^3F)5d$ $^4$F** + 11 $4f^{13}5p^5(^3F)5d$ $^2$G + 8 $4f^{12}5p^6(^3F)5d$ $^4$D |
| 13 | 395,474 | 395,124 | 350 | 1/2 | 38 **$4f^{14}5p^4(^3P)5d$ $^4$P** + 17 $4f^{13}5p^5(^3D)5d$ $^2$S + 8 $4f^{14}5p^4(^3P)5d$ $^2$P |
| 14 | 396,505 | 396,147 | 358 | 7/2 | 20 **$4f^{13}5p^5(^3D)5d$ $^4$F** + 14 $4f^{13}5p^5(^3F)5d$ $^2$G + 8 $4f^{13}5p^5(^3D)5d$ $^2$F |
| 15 | 396,894 | 396,671 | 22 | 3/2 | 17 **$4f^{13}5p^5(^3F)5d$ $^2$P** + 17 $4f^{14}5p^4(^3P)5d$ $^4$P + 16 $4f^{14}5p^4(^3P)5d$ $^4$F |
| 16 | 397,612 | 397,709 | −97 | 5/2 | 19 **$4f^{12}5p^6(^1G)5d$ $^2$D** + 19 $4f^{12}5p^6(^3F)5d$ $^4$D |
| 17 | 398,707 | 398,269 | 438 | 9/2 | 15 **$4f^{13}5p^5(^1G)5d$ $^2$G** + 15 $4f^{13}5p^5(^3G)5d$ $^4$G + 13 $4f^{13}5p^5(^1G)5d$ $^2$H |
| 18 | 400,203 | 400,110 | 93 | 9/2 | 19 **$4f^{12}5p^6(^3F)5d$ $^4$G** + 14 $4f^{12}5p^6(^1G)5d$ $^2$H + 13 $4f^{12}5p^6(^3F)5d$ $^4$F |
| 19 | 401,984 | 402,399 | −415 | 5/2 | 20 **$4f^{14}5p^4(^3P)5d$ $^4$F** + 17 $4f^{13}5p^5(^3G)5d$ $^2$D + 8 $4f^{14}5p^4(^1D)5d$ $^2$F |
| 20 | 405,907 | 405,757 | 150 | 9/2 | 41 **$4f^{12}5p^6(^3H)5d$ $^4$G** + 25 $4f^{12}5p^6(^3H)5d$ $^4$H + 8 $4f^{12}5p^6(^3H)5d$ $^4$F |
| 21 | 408,086 | 407,948 | 138 | 7/2 | 42 **$4f^{12}5p^6(^3H)5d$ $^2$F** + 7 $4f^{12}5p^6(^3F)5d$ $^2$F + 7 $4f^{12}5p^6(^1G)5d$ $^2$F |
| 22 | 408,833 | 409,199 | −366 | 3/2 | 21 **$4f^{12}5p^6(^1G)5d$ $^2$D** + 17 $4f^{12}5p^6(^1D)5d$ $^2$D + 8 $4f^{12}5p^6(^3F)5d$ $^2$D |
| 23 | 409,362 | 409,047 | 315 | 5/2 | 38 **$4f^{12}5p^6(^3H)5d$ $^4$F** + 25 $4f^{12}5p^6(^3F)5d$ $^4$F + 10 $4f^{12}5p^6(^1G)5d$ $^2$D |
| 24 | 409,676 | 409,619 | 57 | 5/2 | 18 **$4f^{12}5p^6(^3F)5d$ $^4$P** + 16 $4f^{12}5p^6(^3F)5d$ $^4$G + 10 $4f^{12}5p^6(^3H)5d$ $^2$F |
| 25 | 410,258 | 409,885 | 373 | 3/2 | 17 **$4f^{12}5p^6(^3F)5d$ $^2$D** + 13 $4f^{13}5p^5(^3G)5d$ $^4$F + 12 $4f^{13}5p^5(^1G)5d$ $^2$D |
| 26 | 410,654 | 410,270 | 384 | 7/2 | 13 **$4f^{12}5p^6(^3F)5d$ $^4$G** + 9 $4f^{12}5p^6(^3H)5d$ $^2$G + 8 $4f^{13}5p^5(^3D)5d$ $^2$G |
| 27 | 411,819 | 412,499 | −680 | 5/2 | 18 **$4f^{12}5p^6(^3H)5d$ $^2$F** + 10 $4f^{13}5p^5(^3G)5d$ $^4$G + 10 $4f^{12}5p^6(^3F)5d$ $^4$G |
| 28 | 411,832 | 411,499 | 333 | 7/2 | 23 **$4f^{12}5p^6(^3F)5d$ $^4$D** + 21 $4f^{12}5p^6(^3F)5d$ $^4$H + 14 $4f^{12}5p^6(^1G)5d$ $^2$G |
| 29 | 413,450 | 413,503 | −53 | 9/2 | 28 **$4f^{12}5p^6(^3H)5d$ $^2$G** + 13 $4f^{12}5p^6(^3F)5d$ $^4$H + 12 $4f^{12}5p^6(^3H)5d$ $^4$I |
| 30 | 414,888 | 414,853 | 35 | 7/2 | 39 **$4f^{12}5p^6(^3F)5d$ $^4$G** + 11 $4f^{12}5p^6(^3F)5d$ $^2$F + 10 $4f^{12}5p^6(^3F)5d$ $^4$H |
| 31 | 415,852 | 415,874 | −22 | 5/2 | 27 **$4f^{12}5p^6(^3F)5d$ $^4$G** + 16 $4f^{12}5p^6(^1G)5d$ $^2$F + 13 $4f^{12}5p^6(^3F)5d$ $^4$P |
| 32 | 416,481 | 416,737 | −256 | 9/2 | 29 **$4f^{12}5p^6(^3F)5d$ $^2$G** + 18 $4f^{12}5p^6(^3H)5d$ $^4$I + 10 $4f^{12}5p^6(^1G)5d$ $^2$G |
| 33 | 417,394 | 417,333 | 61 | 3/2 | 42 **$4f^{12}5p^6(^3F)5d$ $^2$P** + 16 $4f^{12}5p^6(^1G)5d$ $^2$D |
| 34 | 418,403 | 418,274 | 129 | 9/2 | 28 **$4f^{12}5p^6(^3F)5d$ $^4$H** + 28 $4f^{12}5p^6(^3H)5d$ $^2$G + 18 $4f^{12}5p^6(^3H)5d$ $^4$G |
| 35 | 419,585 | 419,953 | −368 | 7/2 | 35 **$4f^{12}5p^6(^3H)5d$ $^4$G** + 11 $4f^{12}5p^6(^3F)5d$ $^4$F + 10 $4f^{12}5p^6(^3H)5d$ $^4$F |

**Table 2.** *Cont.*

| Index | $E_{exp}$ [a] | $E_{calc}$ [b] | ΔE [c] | J | Percentage Composition in LS-Coupling [d] |
|---|---|---|---|---|---|
| 36 | 419,811 | 419,829 | −18 | 5/2 | 25 **$4f^{12}5p^6(^3H)5d\ ^4F$** + 14 $4f^{12}5p^6(^3H)5d\ ^2F$ |
| 37 | 424,781 | 424,776 | 5 | 5/2 | 26 **$4f^{12}5p^6(^3H)5d\ ^4G$** + 19 $4f^{12}5p^6(^3F)5d\ ^4P$ + 15 $4f^{12}5p^6(^1G)5d\ ^2D$ |
| 38 | 425,843 | 425,913 | −70 | 3/2 | 38 **$4f^{12}5p^6(^3H)5d\ ^4F$** + 27 $4f^{12}5p^6(^3F)5d\ ^2P$ + 11 $4f^{12}5p^6(^3F)5d\ ^4P$ |
| 39 | 428,199 | 427,900 | 299 | 3/2 | 42 **$4f^{12}5p^6(^3F)5d\ ^4P$** + 11 $4f^{12}5p^6(^3H)5d\ ^4F$ + 6 $4f^{12}5p^6(^3F)5d\ ^2P$ |
| 40 | 428,216 | 428,371 | −155 | 7/2 | 30 **$4f^{12}5p^6(^3F)5d\ ^2G$** + 10 $4f^{12}5p^6(^3H)5d\ ^2F$ + 7 $4f^{12}5p^6(^3H)5d\ ^2G$ |
| 41 | 428,777 | 428,727 | 50 | 7/2 | 26 **$4f^{12}5p^6(^3F)5d\ ^2F$** + 17 $4f^{12}5p^6(^3F)5d\ ^4F$ + 11 $4f^{12}5p^6(^3H)5d\ ^4H$ |
| 42 | 430,708 | 430,640 | 68 | 7/2 | 20 **$4f^{14}5p^4(^3P)5d\ ^4F$** + 16 $4f^{12}5p^6(^1G)5d\ ^2F$ + 10 $4f^{12}5p^6(^3H)5d\ ^4H$ |
| 43 | 432,963 | 433,564 | −601 | 5/2 | 13 **$4f^{12}5p^6(^3P)5d\ ^4D$** + 10 $4f^{14}5p^4(^3P)5d\ ^4F$ + 9 $4f^{14}5p^4(^1D)5d\ ^2F$ |
| 44 | 435,561 | 435,879 | −318 | 5/2 | 15 **$4f^{12}5p^6(^1D)5d\ ^2F$** + 14 $4f^{12}5p^6(^1G)5d\ ^2D$ + 8 $4f^{14}5p^4(^1D)5d\ ^2F$ |
| 45 | 435,658 | 435,516 | 142 | 7/2 | 14 **$4f^{12}5p^6(^3H)5d\ ^2G$** + 12 $4f^{12}5p^6(^1G)5d\ ^2G$ |
| 46 | 437,149 | 437,658 | −509 | 5/2 | 14 **$4f^{12}5p^6(^3H)5d\ ^2F$** + 14 $4f^{12}5p^6(^3H)5d\ ^4G$ + 11 $4f^{12}5p^6(^1G)5d\ ^2D$ |
| 47 | 439,561 | 439,318 | 243 | 7/2 | 15 **$4f^{12}5p^6(^3H)5d\ ^2G$** + 13 $4f^{12}5p^6(^3P)5d\ ^2F$ + 12 $4f^{12}5p^6(^1G)5d\ ^2F$ |
| 48 | 445,286 | 445,209 | 77 | 5/2 | 15 **$4f^{12}5p^6(^3P)5d\ ^2D$** + 13 $4f^{12}5p^6(^1D)5d\ ^2D$ + 5 $4f^{14}5p^4(^1D)5d\ ^2D$ |
| 49 | 447,909 | 447,860 | 49 | 5/2 | 19 **$4f^{12}5p^6(^1G)5d\ ^2F$** + 14 $4f^{12}5p^6(^3P)5d\ ^4D$ + 13 $4f^{12}5p^6(^3F)5d\ ^2F$ |
| 50 | 452,821 | 452,511 | 310 | 3/2 | 24 **$4f^{12}5p^6(^3P)5d\ ^4P$** + 11 $4f^{13}5p^5(^1G)5d\ ^2D$ + 10 $4f^{12}5p^6(^3P)5d\ ^2P$ |
| 51 | 454,067 | 454,016 | 51 | 7/2 | 66 **$4f^{12}5p^6(^1I)5d\ ^2G$** + 7 $4f^{13}5p^5(^3G)5d\ ^4H$ + 5 $4f^{12}5p^6(^3H)5d\ ^2G$ |
| 52 | 457,652 | 457,245 | 407 | 5/2 | 17 **$4f^{13}5p^5(^1G)5d\ ^2F$** + 14 $4f^{13}5p^5(^3G)5d\ ^2F$ + 9 $4f^{12}5p^6(^1D)5d\ ^2D$ |
| 53 | 457,815 | 457,776 | 39 | 9/2 | 64 **$4f^{12}5p^6(^1I)5d\ ^2H$** + 7 $4f^{13}5p^5(^1G)5d\ ^2G$ + 6 $4f^{13}5p^5(^3D)5d\ ^2G$ |
| 54 | 458,380 | 458,337 | 43 | 3/2 | 16 **$4f^{12}5p^6(^3P)5d\ ^2P$** + 12 $4f^{12}5p^6(^3P)5d\ ^4P$ |
| 55 | 459,570 | 460,304 | −734 | 5/2 | 22 **$4f^{12}5p^6(^3P)5d\ ^2D$** + 6 $4f^{12}5p^6(^3P)5d\ ^2F$ |
| 56 | 462,927 | 463,121 | −194 | 3/2 | 24 **$4f^{12}5p^6(^3P)5d\ ^2D$** + 14 $4f^{13}5p^5(^1D)5d\ ^2D$ + 10 $4f^{13}5p^5(^3F)5d\ ^4F$ |
| 57 | 466,219 | 466,223 | −4 | 5/2 | 33 **$4f^{12}5p^6(^3P)5d\ ^2F$** + 10 $4f^{12}5p^6(^1D)5d\ ^2D$ + 7 $4f^{12}5p^6(^3P)5d\ ^4F$ |
| 58 | 468,034 | 467,620 | 414 | 5/2 | 23 **$4f^{12}5p^6(^3P)5d\ ^2F$** + 9 $4f^{13}5p^5(^1D)5d\ ^2F$ + 6 $4f^{13}5p^5(^3F)5d\ ^4G$ |
| 59 | 468,523 | 468,312 | 211 | 5/2 | 52 **$4f^{12}5p^6(^3P)5d\ ^4P$** + 5 $4f^{12}5p^6(^1D)5d\ ^2D$ + 5 $4f^{13}5p^5(^3G)5d\ ^4F$ |
| 60 | 475,117 | 475,279 | −162 | 3/2 | 15 **$4f^{14}5p^4(^1D)5d\ ^2P$** + 9 $4f^{14}5p^4(^3P)5d\ ^4F$ |
| 61 | 481,035 | 480,441 | 594 | 5/2 | 26 **$4f^{14}5p^4(^3P)5d\ ^2D$** + 16 $4f^{14}5p^4(^1D)5d\ ^2D$ + 9 $4f^{13}5p^5(^1D)5d\ ^2D$ |
| 62 | 481,473 | 481,921 | −448 | 5/2 | 65 **$4f^{14}5p^4(^3P)6s\ ^4P$** + 23 $4f^{14}5p^4(^1D)6s\ ^2D$ |
| 63 | 483,243 | 483,385 | −142 | 3/2 | 18 **$4f^{13}5p^5(^1D)5d\ ^2P$** + 16 $4f^{14}5p^4(^1D)5d\ ^2P$ |
| 64 | 485,175 | 486,300 | −1125 | 5/2 | 22 **$4f^{13}5p^5(^1D)5d\ ^2D$** + 11 $4f^{13}5p^5(^1D)5d\ ^2F$ + 7 $4f^{13}5p^5(^3F)5d\ ^4F$ |
| 65 | 487,901 | 487,064 | 837 | 3/2 | 50 **$4f^{14}5p^4(^3P)6s\ ^2P$** + 27 $4f^{14}5p^4(^1D)6s\ ^2D$ + 13 $4f^{14}5p^4(^3P)6s\ ^4P$ |
| 66 | 492,337 | 493,284 | −947 | 1/2 | 32 **$4f^{14}5p^4(^1D)5d\ ^2P$** + 21 $4f^{14}5p^4(^1D)5d\ ^2S$ + 16 $4f^{14}5p^4(^3P)5d\ ^2P$ |
| 67 | 495,690 | 495,041 | 649 | 9/2 | 27 **$4f^{13}5p^5(^3D)5d\ ^2G$** + 18 $4f^{13}5p^5(^3F)5d\ ^2G$ + 10 $4f^{13}5p^5(^3G)5d\ ^2G$ |
| 68 | 498,037 | 499,096 | −1059 | 5/2 | 29 **$4f^{13}5p^5(^3G)5d\ ^2D$** + 14 $4f^{13}5p^5(^1G)5d\ ^2D$ + 9 $4f^{12}5p^6(^3P)5d\ ^2D$ |
| 69 | 498,541 | 498,826 | −285 | 3/2 | 26 **$4f^{14}5p^4(^1D)5d\ ^2D$** + 13 $4f^{12}5p^6(^1S)5d\ ^2D$ + 10 $4f^{14}5p^4(^3P)5d\ ^2D$ |
| 70 | 498,792 | 499,045 | −253 | 7/2 | 18 **$4f^{13}5p^5(^3G)5d\ ^2F$** + 15 $4f^{13}5p^5(^3F)5d\ ^2F$ + 13 $4f^{13}5p^5(^1G)5d\ ^2F$ |
| 71 | 500,313 | 500,013 | 300 | 5/2 | 56 **$4f^{13}5p^5(^1F)6s\ ^2F$** + 19 $4f^{13}5p^5(^3D)6s\ ^2D$ + 11 $4f^{13}5p^5(^3D)6s\ ^4D$ |
| 72 | 503,071 | 502,605 | 466 | 7/2 | 47 **$4f^{13}5p^5(^3F)6s\ ^2F$** + 16 $4f^{13}5p^5(^1F)6s\ ^2F$ + 10 $4f^{13}5p^5(^3F)6s\ ^4F$ |
| 73 | 504,615 | 504,586 | 29 | 9/2 | 71 **$4f^{13}5p^5(^3G)6s\ ^2G$** + 24 $4f^{13}5p^5(^3G)6s\ ^4G$ |
| 74 | 504,691 | 505,845 | −1154 | 3/2 | 32 **$4f^{12}5p^6(^1S)5d\ ^2D$** + 14 $4f^{13}5p^5(^3G)5d\ ^2D$ + 7 $4f^{13}5p^5(^3F)5d\ ^2D$ |
| 75 | 512,790 | 512,628 | 162 | 7/2 | 17 **$4f^{13}5p^5(^1D)5d\ ^2G$** + 15 $4f^{13}5p^5(^3F)5d\ ^2G$ + 14 $4f^{13}5p^5(^3G)5d\ ^2G$ |
| 76 | 514,063 | 514,203 | −140 | 5/2 | 49 **$4f^{13}5p^5(^1D)6s\ ^2D$** + 26 $4f^{13}5p^5(^3D)6s\ ^4D$ + 10 $4f^{13}5p^5(^3D)6s\ ^2D$ |
| 77 | 514,413 | 514,677 | −264 | 7/2 | 37 **$4f^{13}5p^5(^3F)6s\ ^4F$** + 22 $4f^{13}5p^5(^3F)6s\ ^2F$ + 15 $4f^{13}5p^5(^1F)6s\ ^2F$ |
| 78 | 514,628 | 515,153 | −525 | 5/2 | 50 **$4f^{13}5p^5(^3F)6s\ ^4F$** + 16 $4f^{13}5p^5(^3G)6s\ ^4G$ + 14 $4f^{13}5p^5(^1F)6s\ ^2F$ |
| 79 | 516,493 | 515,725 | 768 | 5/2 | 24 **$4f^{13}5p^5(^3G)5d\ ^2F$** + 14 $4f^{13}5p^5(^3F)5d\ ^2F$ + 11 $4f^{13}5p^5(^1D)5d\ ^2F$ |

**Table 2.** *Cont.*

| Index | $E_{exp}$ [a] | $E_{calc}$ [b] | ΔE [c] | J | Percentage Composition in LS-Coupling [d] |
|---|---|---|---|---|---|
| 80 | 521,876 | 522,299 | −423 | 5/2 | 35 **$4f^{12}5p^6(^1S)5d\ ^2D$** + 26 $4f^{13}5p^5(^3F)6s\ ^2F$ + 10 $4f^{13}5p^5(^3D)6s\ ^4D$ |
| 81 | 522,610 | 521,487 | 1123 | 5/2 | 36 **$4f^{12}5p^6(^1S)5d\ ^2D$** + 25 $4f^{13}5p^5(^3F)6s\ ^2F$ + 10 $4f^{13}5p^5(^3D)6s\ ^4D$ |
| 82 | 522,881 | 522,986 | −105 | 3/2 | 41 **$4f^{12}5p^6(^1S)5d\ ^2D$** + 26 $4f^{13}5p^5(^3G)5d\ ^2D$ + 7 $4f^{12}5p^6(^3P)5d\ ^2D$ |
| 83 | 527,376 | 527,853 | −477 | 7/2 | 46 **$4f^{13}5p^5(^1G)6s\ ^2G$** + 29 $4f^{13}5p^5(^3G)6s\ ^4G$ + 23 $4f^{13}5p^5(^3G)6s\ ^2G$ |
| 84 | 528,462 | 528,388 | 74 | 1/2 | 28 **$4f^{14}5p^4(^1D)5d\ ^2S$** + 17 $4f^{14}5p^4(^3P)5d\ ^2P$ + 8 $4f^{13}5p^5(^3D)5d\ ^2S$ |
| 85 | 528,652 | 528,582 | 70 | 3/2 | 65 **$4f^{13}5p^5(^3D)6s\ ^2D$** + 30 $4f^{13}5p^5(^3D)6s\ ^4D$ |
| 86 | 567,191 | 565,985 | 1206 | 3/2 | 28 **$4f^{14}5p^4(^3P)5d\ ^2D$** + 28 $4f^{14}5p^4(^1S)5d\ ^2D$ + 10 $4f^{14}5p^4(^3P)5d\ ^2P$ |
| 87 | 568,644 | 567,872 | 772 | 3/2 | 77 **$4f^{14}5p^4(^3P)6s\ ^4P$** + 13 $4f^{14}5p^4(^3P)6s\ ^2P$ |
| 88 | 572,004 | 572,684 | −680 | 1/2 | 66 **$4f^{14}5p^4(^3P)6s\ ^2P$** + 32 $4f^{14}5p^4(^3P)6s\ ^4P$ |
| 89 | 581,635 | 582,142 | −507 | 5/2 | 60 **$4f^{14}5p^4(^1D)6s\ ^2D$** + 18 $4f^{14}5p^4(^3P)6s\ ^4P$ + 7 $4f^{12}5p^6(^3F)6s\ ^2F$ |
| 90 | 583,560 | 583,744 | −184 | 3/2 | 60 **$4f^{14}5p^4(^1D)6s\ ^2D$** + 23 $4f^{14}5p^4(^3P)6s\ ^2P$ + 8 $4f^{12}5p^6(^3F)6s\ ^4F$ |
| 91 | 594,941 | 594,876 | 65 | 7/2 | 56 **$4f^{13}5p^5(^3D)6s\ ^4D$** + 23 $4f^{13}5p^5(^3F)6s\ ^4F$ + 11 $4f^{13}5p^5(^1F)6s\ ^2F$ |
| 92 | 597,436 | 597,803 | −367 | 5/2 | 49 **$4f^{13}5p^5(^3D)6s\ ^2D$** + 14 $4f^{13}5p^5(^3F)6s\ ^4F$ + 13 $4f^{13}5p^5(^3D)6s\ ^4D$ |
| 93 | 598,904 | 598,949 | −45 | 7/2 | 39 **$4f^{13}5p^5(^1G)6s\ ^2G$** + 21 $4f^{13}5p^5(^3F)6s\ ^2F$ + 20 $4f^{13}5p^5(^3G)6s\ ^4G$ |
| 94 | 599,423 | 599,274 | 149 | 9/2 | 44 **$4f^{13}5p^5(^1G)6s\ ^2G$** + 25 $4f^{13}5p^5(^3G)6s\ ^4G$ + 19 $4f^{13}5p^5(^3F)6s\ ^4F$ |
| 95 | 609,206 | 609,104 | 102 | 5/2 | 73 **$4f^{13}5p^5(^3G)6s\ ^4G$** + 18 $4f^{13}5p^5(^1F)6s\ ^2F$ |
| 96 | 611,283 | 611,555 | −272 | 7/2 | 50 **$4f^{13}5p^5(^3G)6s\ ^2G$** + 27 $4f^{13}5p^5(^3G)6s\ ^4G$ + 16 $4f^{13}5p^5(^1F)6s\ ^2F$ |
| 97 | 621,343 | 620,931 | 412 | 5/2 | 39 **$4f^{13}5p^5(^1D)6s\ ^2D$** + 19 $4f^{13}5p^5(^3F)6s\ ^2F$ + 14 $4f^{13}5p^5(^3D)6s\ ^4D$ |
| 98 | 622,123 | 621,607 | 516 | 3/2 | 40 **$4f^{13}5p^5(^1D)6s\ ^2D$** + 28 $4f^{13}5p^5(^3F)6s\ ^4F$ + 9 $4f^{13}5p^5(^3D)6s\ ^4D$ |

[a] From [13]. [b] This work : model HFR(F). [c] $\Delta E = E_{exp} - E_{calc}$. [d] Only the first three *LS* components larger then 5% are given.

The calculated oscillator strengths (log *gf*) and transition probabilities (*gA*) obtained in the present work are given in Table 3 for all the W VIII spectral lines with log gf-values greater than −4. These parameters are only given in the length form, the HFR code of Cowan not allowing the calculation of radiative decay rates in the velocity form. Observed wavelengths ($ë_{exp}$) taken from the work of Ryabtsev *et al.* [13] are also given in the same table together with the 'Ritz' wavelengths ($\lambda_{Ritz}$) deduced from the experimental energy levels identified by the same authors. When looking in detail at the table, one can see that forty listed lines were not observed in [13]. If most of those lines are characterized by rather weak transition probabilities, three of them appear to be strong enough, *i.e.*, with gA-values greater than $10^{10}$ $s^{-1}$, to be experimentally observed, according to our calculations. These are located at λ = 191.700 Å (gA = 1.46 × $10^{10}$ $s^{-1}$), λ = 229.402 Å (gA = 1.16 × $10^{10}$ $s^{-1}$) and λ = 244.249 Å (gA = 1.33 × $10^{11}$ $s^{-1}$) and correspond respectively to transitions from the lower odd level at 1233 $cm^{-1}$ (J = 3/2), to the upper even level at 522,881 $cm^{-1}$ (J = 3/2), from the lower odd level at 1233 $cm^{-1}$ (J = 3/2) to the upper even level at 437,149 $cm^{-1}$ (J = 5/2), and from the lower odd level at 89,123 $cm^{-1}$ (J = 1/2) to the upper even level at 498,541 $cm^{-1}$ (J = 3/2).

**Table 3.** Oscillator strengths and transition probabilities in W VIII (log gf > −4). A table entry 6.81E + 08 means $6.81\times10^{8}$.

| Indexes [a] | Wavelength [b] | | Lower Odd Level [c] | | Upper Even Level [c] | | | | |
|---|---|---|---|---|---|---|---|---|---|
| | $\lambda_{exp}$ (Å) | $\lambda_{Ritz}$ (Å) | E ($cm^{-1}$) | J | E ($cm^{-1}$) | J | log gf [d] | gA ($s^{-1}$) [d] | CF [e] |
| 1° − 97 | 160.940 | 160.942 | 0 | 3.5 | 621,343 | 2.5 | −2.58 | 6.81E + 08 | 0.003 |
| 2° − 98 | 161.057 | 161.059 | 1233 | 1.5 | 622,123 | 1.5 | −2.41 | 1.01E + 09 | 0.045 |
| 2° − 97 | 161.260 | 161.262 | 1233 | 1.5 | 621,343 | 2.5 | −1.26 | 1.40E + 10 | 0.333 |
| 1° − 96 | 163.596 | 163.590 | 0 | 3.5 | 611,283 | 3.5 | −2.30 | 1.24E + 09 | 0.007 |
| 1° − 95 | 164.143 | 164.148 | 0 | 3.5 | 609,206 | 2.5 | −2.78 | 4.15E + 08 | 0.014 |
| 2° − 95 | 164.479 | 164.481 | 1233 | 1.5 | 609,206 | 2.5 | −3.29 | 1.27E + 08 | 0.226 |
| 3° − 98 | 165.369 | 165.368 | 17,410 | 2.5 | 622,123 | 1.5 | −0.26 | 1.34E + 11 | 0.854 |
| 3° − 97 | 165.583 | 165.581 | 17,410 | 2.5 | 621,343 | 2.5 | −0.42 | 9.25E + 10 | 0.609 |
| 1° − 94 | 166.827 | 166.827 | 0 | 3.5 | 599,423 | 4.5 | 0.15 | 3.39E + 11 | 0.872 |
| 1° − 93 | 166.971 | 166.972 | 0 | 3.5 | 598,904 | 3.5 | −0.22 | 1.44E + 11 | 0.558 |
| 1° − 92 | 167.382 | 167.382 | 0 | 3.5 | 597,436 | 2.5 | −0.04 | 2.16E + 11 | 0.721 |
| 1° − 91 | 168.084 | 168.084 | 0 | 3.5 | 594,941 | 3.5 | −0.56 | 6.57E + 10 | 0.820 |
| 3° − 96 | 168.381 | 168.386 | 17,410 | 2.5 | 611,283 | 3.5 | 0.05 | 2.62E + 11 | 0.730 |
| 3° − 95 | 168.980 | 168.977 | 17,410 | 2.5 | 609,206 | 2.5 | −0.59 | 6.03E + 10 | 0.778 |
| 2° − 90 | 171.727 | 171.725 | 1233 | 1.5 | 583,560 | 1.5 | −0.80 | 3.56E + 10 | 0.131 |
| 1° − 89 | | 171.929 | 0 | 3.5 | 581,635 | 2.5 | −2.76 | 3.98E + 08 | 0.038 |
| 3° − 93 | 171.973 | 171.971 | 17,410 | 2.5 | 598,904 | 3.5 | −1.70 | 4.48E + 09 | 0.013 |
| 2° − 89 | 172.295 | 172.294 | 1233 | 1.5 | 581,635 | 2.5 | −0.19 | 1.46E + 11 | 0.641 |
| 3° − 91 | | 173.151 | 17,410 | 2.5 | 594,941 | 3.5 | −2.67 | 4.74E + 08 | 0.026 |
| 2° − 88 | 175.199 | 175.202 | 1233 | 1.5 | 572,004 | 0.5 | −0.58 | 5.76E + 10 | 0.632 |
| 2° − 87 | 176.237 | 176.239 | 1233 | 1.5 | 568,644 | 1.5 | −0.80 | 3.38E + 10 | 0.039 |
| 3° − 90 | 176.630 | 176.632 | 17,410 | 2.5 | 583,560 | 1.5 | −1.27 | 1.15E + 10 | 0.701 |
| 2° − 86 | 176.694 | 176.692 | 1233 | 1.5 | 567,191 | 1.5 | −0.75 | 3.77E + 10 | 0.030 |
| 3° − 89 | 177.232 | 177.234 | 17,410 | 2.5 | 581,635 | 2.5 | −1.36 | 9.27E + 09 | 0.591 |
| 3° − 87 | 181.410 | 181.411 | 17,410 | 2.5 | 568,644 | 1.5 | −1.07 | 1.74E + 10 | 0.134 |
| 3° − 86 | 181.888 | 181.891 | 17,410 | 2.5 | 567,191 | 1.5 | −0.67 | 4.28E + 10 | 0.176 |
| 4° − 98 | 187.608 | 187.617 | 89,123 | 0.5 | 622,123 | 1.5 | −1.50 | 5.93E + 09 | 0.256 |
| 2° − 85 | | 189.603 | 1233 | 1.5 | 528,652 | 1.5 | −2.44 | 6.70E + 08 | 0.083 |
| 1° − 83 | 189.616 | 189.618 | 0 | 3.5 | 527,376 | 3.5 | −1.17 | 1.25E + 10 | 0.452 |
| 2° − 84 | 189.667 | 189.671 | 1233 | 1.5 | 528,462 | 0.5 | −0.59 | 4.81E + 10 | 0.030 |
| 1° − 81 | 191.348 | 191.347 | 0 | 3.5 | 522,610 | 2.5 | −0.67 | 3.89E + 10 | 0.082 |
| 1° − 80 | 191.617 | 191.616 | 0 | 3.5 | 521,876 | 2.5 | −0.46 | 6.38E + 10 | 0.102 |
| 2° − 82 | | 191.700 | 1233 | 1.5 | 522,881 | 1.5 | −1.10 | 1.46E + 10 | 0.069 |
| 2° − 81 | | 191.800 | 1233 | 1.5 | 522,610 | 2.5 | −3.00 | 1.78E + 08 | 0.001 |
| 2° − 80 | 192.070 | 192.070 | 1233 | 1.5 | 521,876 | 2.5 | −2.25 | 1.02E + 09 | 0.007 |
| 1° − 79 | 193.614 | 193.613 | 0 | 3.5 | 516,493 | 2.5 | −0.96 | 1.95E + 10 | 0.029 |
| 2° − 79 | 194.077 | 194.077 | 1233 | 1.5 | 516,493 | 2.5 | −1.37 | 7.51E + 09 | 0.095 |
| 1° − 78 | 194.315 | 194.315 | 0 | 3.5 | 514,628 | 2.5 | −2.94 | 2.05E + 08 | 0.011 |
| 1° − 77 | 194.397 | 194.396 | 0 | 3.5 | 514,413 | 3.5 | −0.59 | 4.58E + 10 | 0.047 |
| 1° − 76 | 194.527 | 194.529 | 0 | 3.5 | 514,063 | 2.5 | 0.09 | 2.19E + 11 | 0.840 |
| 2° − 76 | 194.998 | 194.996 | 1233 | 1.5 | 514,063 | 2.5 | −1.46 | 6.02E + 09 | 0.403 |
| 1° − 75 | 195.021 | 195.012 | 0 | 3.5 | 512,790 | 3.5 | −1.64 | 4.01E + 09 | 0.003 |

**Table 3.** *Cont.*

| Indexes [a] | Wavelength [b] | | Lower Odd Level [c] | | Upper Even Level [c] | | | | |
|---|---|---|---|---|---|---|---|---|---|
| | $\lambda_{exp}$ (Å) | $\lambda_{Ritz}$ (Å) | E ($cm^{-1}$) | J | E ($cm^{-1}$) | J | log gf [d] | gA ($s^{-1}$) [d] | CF [e] |
| 3° − 85 | 195.598 | 195.602 | 17,410 | 2.5 | 528,652 | 1.5 | 0.10 | 2.19E + 11 | 0.790 |
| 3° − 83 | 196.093 | 196.092 | 17,410 | 2.5 | 527,376 | 3.5 | 0.20 | 2.76E + 11 | 0.866 |
| 3° − 82 | 197.835 | 197.835 | 17,410 | 2.5 | 522,881 | 1.5 | 0.63 | 7.37E + 11 | 0.514 |
| 3° − 81 | 197.941 | 197.941 | 17,410 | 2.5 | 522,610 | 2.5 | −1.91 | 2.07E + 09 | 0.005 |
| 1° − 73 | 198.171 | 198.171 | 0 | 3.5 | 504,615 | 4.5 | 0.46 | 4.87E + 11 | 0.850 |
| 3° − 80 | 198.229 | 198.229 | 17,410 | 2.5 | 521,876 | 2.5 | 0.49 | 5.31E + 11 | 0.659 |
| 1° − 72 | 198.779 | 198.779 | 0 | 3.5 | 503,071 | 3.5 | 0.67 | 7.94E + 11 | 0.742 |
| 1° − 71 | 199.875 | 199.875 | 0 | 3.5 | 500,313 | 2.5 | −1.02 | 1.58E + 10 | 0.098 |
| 3° − 79 | 200.367 | 200.367 | 17,410 | 2.5 | 516,493 | 2.5 | 1.04 | 1.82E + 12 | 0.555 |
| 2° − 71 | | 200.369 | 1233 | 1.5 | 500,313 | 2.5 | −2.31 | 8.23E + 08 | 0.183 |
| 1° − 70 | 200.483 | 200.484 | 0 | 3.5 | 498,792 | 3.5 | 1.14 | 2.31E + 12 | 0.467 |
| 1° − 68 | 200.787 | 200.788 | 0 | 3.5 | 498,037 | 2.5 | 1.05 | 1.90E + 12 | 0.572 |
| 2° − 69 | 201.079 | 201.083 | 1233 | 1.5 | 498,541 | 1.5 | 0.09 | 2.05E + 11 | 0.358 |
| 3° − 78 | 201.119 | 201.119 | 17,410 | 2.5 | 514,628 | 2.5 | −0.85 | 2.33E + 10 | 0.219 |
| 3° − 77 | 201.205 | 201.206 | 17,410 | 2.5 | 514,413 | 3.5 | 0.83 | 1.13E + 12 | 0.562 |
| 2° − 68 | 201.288 | 201.287 | 1233 | 1.5 | 498,037 | 2.5 | 0.12 | 2.17E + 11 | 0.196 |
| 3° − 76 | | 201.348 | 17,410 | 2.5 | 514,063 | 2.5 | −2.01 | 1.61E + 09 | 0.026 |
| 1° − 67 | 201.739 | 201.739 | 0 | 3.5 | 495,690 | 4.5 | 1.29 | 3.22E + 12 | 0.577 |
| 3° − 75 | 201.864 | 201.865 | 17,410 | 2.5 | 512,790 | 3.5 | 0.98 | 1.56E + 12 | 0.446 |
| 4° − 90 | 202.250 | 202.250 | 89,123 | 0.5 | 583,560 | 1.5 | −0.07 | 1.39E + 11 | 0.835 |
| 2° − 66 | 203.623 | 203.623 | 1233 | 1.5 | 492,337 | 0.5 | 0.62 | 6.72E + 11 | 0.563 |
| 3° − 74 | 205.221 | 205.220 | 17,410 | 2.5 | 504,691 | 1.5 | 0.53 | 5.37E + 11 | 0.474 |
| 2° − 65 | 205.479 | 205.479 | 1233 | 1.5 | 487,901 | 1.5 | 0.32 | 3.29E + 11 | 0.754 |
| 3° − 72 | | 205.905 | 17,410 | 2.5 | 503,071 | 3.5 | −3.56 | 4.31E + 07 | 0.000 |
| 1° − 64 | | 206.111 | 0 | 3.5 | 485,175 | 2.5 | −1.20 | 9.98E + 09 | 0.028 |
| 2° − 64 | 206.634 | 206.636 | 1233 | 1.5 | 485,175 | 2.5 | 0.29 | 3.08E + 11 | 0.518 |
| 3° − 71 | | 207.081 | 17,410 | 2.5 | 500,313 | 2.5 | −1.64 | 3.56E + 09 | 0.020 |
| 4° − 88 | 207.092 | 207.090 | 89,123 | 0.5 | 572,004 | 0.5 | −0.31 | 7.59E + 10 | 0.784 |
| 2° − 63 | 207.466 | 207.465 | 1233 | 1.5 | 483,243 | 1.5 | 0.27 | 2.86E + 11 | 0.266 |
| 1° − 62 | 207.690 | 207.696 | 0 | 3.5 | 481,473 | 2.5 | −0.69 | 3.20E + 10 | 0.364 |
| 3° − 70 | 207.736 | 207.735 | 17,410 | 2.5 | 498,792 | 3.5 | −0.80 | 2.49E + 10 | 0.027 |
| 3° − 69 | 207.850 | 207.844 | 17,410 | 2.5 | 498,541 | 1.5 | −1.23 | 9.15E + 09 | 0.025 |
| 1° − 61 | 207.884 | 207.885 | 0 | 3.5 | 481,035 | 2.5 | −0.37 | 6.55E + 10 | 0.216 |
| 3° − 68 | | 208.062 | 17,410 | 2.5 | 498,037 | 2.5 | −3.79 | 2.56E + 07 | 0.000 |
| 2° − 62 | 208.227 | 208.229 | 1233 | 1.5 | 481,473 | 2.5 | −0.21 | 9.49E + 10 | 0.160 |
| 2° − 61 | 208.420 | 208.419 | 1233 | 1.5 | 481,035 | 2.5 | 0.83 | 1.04E + 12 | 0.638 |
| 4° − 87 | 208.543 | 208.541 | 89,123 | 0.5 | 568,644 | 1.5 | 0.42 | 4.04E + 11 | 0.534 |
| 4° − 86 | 209.175 | 209.175 | 89,123 | 0.5 | 567,191 | 1.5 | 0.62 | 6.31E + 11 | 0.502 |
| 2° − 60 | 211.027 | 211.022 | 1233 | 1.5 | 475,117 | 1.5 | 0.28 | 2.87E + 11 | 0.369 |
| 1° − 59 | 213.436 | 213.437 | 0 | 3.5 | 468,523 | 2.5 | −2.91 | 1.81E + 08 | 0.001 |
| 1° − 58 | 213.661 | 213.660 | 0 | 3.5 | 468,034 | 2.5 | −3.04 | 1.33E + 08 | 0.000 |
| 3° − 64 | 213.785 | 213.783 | 17,410 | 2.5 | 485,175 | 2.5 | −1.03 | 1.36E + 10 | 0.024 |
| 2° − 59 | 214.001 | 214.000 | 1233 | 1.5 | 468,523 | 2.5 | −2.50 | 4.61E + 09 | 0.013 |

**Table 3.** *Cont.*

| Indexes [a] | Wavelength [b] | | Lower Odd Level [c] | | Upper Even Level [c] | | | | |
|---|---|---|---|---|---|---|---|---|---|
| | $\lambda_{exp}$ (Å) | $\lambda_{Ritz}$ (Å) | E ($cm^{-1}$) | J | E ($cm^{-1}$) | J | log gf [d] | gA ($s^{-1}$) [d] | CF [e] |
| 2° − 58 | 214.229 | 214.224 | 1233 | 1.5 | 468,034 | 2.5 | −0.09 | 1.17E + 11 | 0.428 |
| 1° − 57 | 214.488 | 214.491 | 0 | 3.5 | 466,219 | 2.5 | −2.31 | 7.13E + 08 | 0.002 |
| 2° − 57 | 215.055 | 215.060 | 1233 | 1.5 | 466,219 | 2.5 | −0.21 | 8.80E + 10 | 0.439 |
| 3° − 62 | 215.496 | 215.488 | 17,410 | 2.5 | 481,473 | 2.5 | −2.22 | 8.60E + 08 | 0.023 |
| 3° − 61 | 215.692 | 215.692 | 17,410 | 2.5 | 481,035 | 2.5 | −1.75 | 2.57E + 09 | 0.012 |
| 2° − 56 | 216.596 | 216.594 | 1233 | 1.5 | 462,927 | 1.5 | −0.71 | 2.79E + 10 | 0.187 |
| 1° − 55 | 217.601 | 217.595 | 0 | 3.5 | 459,570 | 2.5 | −2.39 | 5.78E + 08 | 0.001 |
| 2° − 55 | 218.174 | 218.180 | 1233 | 1.5 | 459,570 | 2.5 | −2.25 | 7.95E + 08 | 0.004 |
| 1° − 53 | 218.429 | 218.429 | 0 | 3.5 | 457,815 | 4.5 | −0.93 | 1.66E + 10 | 0.028 |
| 3° − 60 | 218.477 | 218.480 | 17,410 | 2.5 | 475,117 | 1.5 | −2.25 | 7.91E + 08 | 0.003 |
| 1° − 52 | 218.507 | 218.507 | 0 | 3.5 | 457,652 | 2.5 | −1.24 | 8.04E + 09 | 0.011 |
| 2° − 54 | 218.747 | 218.748 | 1233 | 1.5 | 458,380 | 1.5 | −0.88 | 1.85E + 10 | 0.063 |
| 2° − 52 | 219.097 | 219.097 | 1233 | 1.5 | 457,652 | 2.5 | −2.89 | 1.76E + 08 | 0.002 |
| 1° − 51 | 220.239 | 220.232 | 0 | 3.5 | 454,067 | 3.5 | −3.13 | 1.02E + 08 | 0.000 |
| 2° − 50 | 221.443 | 221.441 | 1233 | 1.5 | 452,821 | 1.5 | −0.49 | 4.43E + 10 | 0.075 |
| 3° − 59 | | 221.674 | 17,410 | 2.5 | 468,523 | 2.5 | −2.13 | 1.01E + 09 | 0.005 |
| 3° − 58 | 221.908 | 221.915 | 17,410 | 2.5 | 468,034 | 2.5 | −0.80 | 2.14E + 10 | 0.030 |
| 3° − 57 | 222.818 | 222.812 | 17,410 | 2.5 | 466,219 | 2.5 | −1.15 | 9.46E + 09 | 0.018 |
| 1° − 49 | 223.260 | 223.260 | 0 | 3.5 | 447,909 | 2.5 | −1.33 | 6.17E + 09 | 0.028 |
| 2° − 49 | | 223.876 | 1233 | 1.5 | 447,909 | 2.5 | −1.59 | 3.39E + 09 | 0.048 |
| 3° − 56 | | 224.458 | 17,410 | 2.5 | 462,927 | 1.5 | −2.63 | 3.12E + 08 | 0.002 |
| 1° − 48 | 224.573 | 224.575 | 0 | 3.5 | 445,286 | 2.5 | −2.38 | 5.55E + 08 | 0.002 |
| 2° − 48 | 225.203 | 225.198 | 1233 | 1.5 | 445,286 | 2.5 | −1.61 | 3.22E + 09 | 0.026 |
| 3° − 55 | | 226.162 | 17,410 | 2.5 | 459,570 | 2.5 | −3.04 | 1.20E + 08 | 0.000 |
| 3° − 54 | | 226.773 | 17,410 | 2.5 | 458,380 | 1.5 | −2.01 | 1.27E + 09 | 0.003 |
| 3° − 52 | | 227.148 | 17,410 | 2.5 | 457,652 | 2.5 | −2.64 | 2.96E + 08 | 0.000 |
| 1° − 47 | 227.497 | 227.500 | 0 | 3.5 | 439,561 | 3.5 | −0.89 | 1.64E + 10 | 0.091 |
| 4° − 85 | 227.519 | 227.516 | 89,123 | 0.5 | 528,652 | 1.5 | −2.26 | 7.04E + 08 | 0.057 |
| 4° − 84 | 227.617 | 227.615 | 89,123 | 0.5 | 528,462 | 0.5 | 0.57 | 4.79E + 11 | 0.552 |
| 3° − 51 | 229.011 | 229.013 | 17,410 | 2.5 | 454,067 | 3.5 | −0.90 | 1.58E + 10 | 0.023 |
| 2° − 46 | | 229.402 | 1233 | 1.5 | 437,149 | 2.5 | −1.04 | 1.16E + 10 | 0.072 |
| 1° − 45 | 229.541 | 229.538 | 0 | 3.5 | 435,658 | 3.5 | −2.02 | 1.21E + 09 | 0.007 |
| 1° − 44 | 229.590 | 229.589 | 0 | 3.5 | 435,561 | 2.5 | −1.07 | 1.07E + 10 | 0.047 |
| 3° − 50 | 229.666 | 229.668 | 17,410 | 2.5 | 452,821 | 1.5 | −1.53 | 3.67E + 09 | 0.007 |
| 2° − 44 | 230.246 | 230.241 | 1233 | 1.5 | 435,561 | 2.5 | −1.01 | 1.23E + 10 | 0.070 |
| 4° − 82 | 230.544 | 230.543 | 89,123 | 0.5 | 522,881 | 1.5 | −0.60 | 3.17E + 10 | 0.107 |
| 1° − 43 | 230.964 | 230.967 | 0 | 3.5 | 432,963 | 2.5 | −1.44 | 4.60E + 09 | 0.019 |
| 2° − 43 | 231.629 | 231.626 | 1233 | 1.5 | 432,963 | 2.5 | −0.74 | 2.28E + 10 | 0.064 |
| 1° − 42 | 232.176 | 232.176 | 0 | 3.5 | 430,708 | 3.5 | −1.18 | 8.25E + 09 | 0.049 |
| 3° − 49 | 232.288 | 232.289 | 17,410 | 2.5 | 447,909 | 2.5 | −0.84 | 1.80E + 10 | 0.084 |
| 1° − 41 | 233.225 | 233.221 | 0 | 3.5 | 428,777 | 3.5 | −0.81 | 1.89E + 10 | 0.073 |
| 1° − 40 | 233.525 | 233.527 | 0 | 3.5 | 428,216 | 3.5 | −0.49 | 3.93E + 10 | 0.161 |
| 3° − 48 | 233.709 | 233.713 | 17,410 | 2.5 | 445,286 | 2.5 | −0.64 | 2.77E + 10 | 0.122 |

**Table 3.** *Cont.*

| Indexes [a] | Wavelength [b] | | Lower Odd Level [c] | | Upper Even Level [c] | | | | |
|---|---|---|---|---|---|---|---|---|---|
| | $\lambda_{exp}$ (Å) | $\lambda_{Ritz}$ (Å) | E ($cm^{-1}$) | J | E ($cm^{-1}$) | J | log gf [d] | gA ($s^{-1}$) [d] | CF [e] |
| 2° − 39 | | 234.211 | 1233 | 1.5 | 428,199 | 1.5 | −2.99 | 1.25E + 08 | 0.001 |
| 1° − 37 | 235.418 | 235.415 | 0 | 3.5 | 424,781 | 2.5 | −1.23 | 7.03E + 09 | 0.055 |
| 2° − 38 | 235.509 | 235.510 | 1233 | 1.5 | 425,843 | 1.5 | −2.07 | 1.02E + 09 | 0.126 |
| 2° − 37 | | 236.101 | 1233 | 1.5 | 424,781 | 2.5 | −2.88 | 1.59E + 08 | 0.007 |
| 3° − 47 | 236.884 | 236.882 | 17,410 | 2.5 | 439,561 | 3.5 | −1.01 | 1.16E + 10 | 0.040 |
| 1° − 36 | | 238.202 | 0 | 3.5 | 419,811 | 2.5 | −3.32 | 5.62E + 07 | 0.000 |
| 3° − 46 | 238.243 | 238.243 | 17,410 | 2.5 | 437,149 | 2.5 | −0.95 | 1.32E + 10 | 0.063 |
| 1° − 35 | 238.330 | 238.331 | 0 | 3.5 | 419,585 | 3.5 | −2.28 | 6.19E + 08 | 0.010 |
| 2° − 36 | | 238.904 | 1233 | 1.5 | 419,811 | 2.5 | −3.13 | 8.56E + 07 | 0.011 |
| 1° − 34 | 239.004 | 239.004 | 0 | 3.5 | 418,403 | 4.5 | −1.03 | 1.08E + 10 | 0.057 |
| 3° − 45 | 239.089 | 239.093 | 17,410 | 2.5 | 435,658 | 3.5 | −0.59 | 3.01E + 10 | 0.156 |
| 3° − 44 | 239.142 | 239.148 | 17,410 | 2.5 | 435,561 | 2.5 | −1.21 | 7.14E + 09 | 0.035 |
| 1° − 32 | 240.107 | 240.107 | 0 | 3.5 | 416,481 | 4.5 | −0.47 | 3.94E + 10 | 0.240 |
| 2° − 33 | | 240.292 | 1233 | 1.5 | 417,394 | 1.5 | −3.24 | 6.63E + 07 | 0.004 |
| 1° − 31 | 240.468 | 240.470 | 0 | 3.5 | 415,852 | 2.5 | −2.40 | 4.62E + 08 | 0.007 |
| 4° − 74 | 240.634 | 240.635 | 89,123 | 0.5 | 504,691 | 1.5 | −0.35 | 5.14E + 10 | 0.150 |
| 1° − 30 | 241.037 | 241.029 | 0 | 3.5 | 414,888 | 3.5 | −1.21 | 7.09E + 09 | 0.024 |
| 2° − 31 | 241.183 | 241.185 | 1233 | 1.5 | 415,852 | 2.5 | −2.36 | 4.97E + 08 | 0.065 |
| 1° − 29 | 241.867 | 241.867 | 0 | 3.5 | 413,450 | 4.5 | −0.27 | 6.16E + 10 | 0.193 |
| 3° − 42 | | 241.956 | 17,410 | 2.5 | 430,708 | 3.5 | −2.16 | 7.91E + 08 | 0.007 |
| 1° − 28 | 242.819 | 242.817 | 0 | 3.5 | 411,832 | 3.5 | −1.36 | 4.97E + 09 | 0.071 |
| 1° − 27 | 242.829 | 242.825 | 0 | 3.5 | 411,819 | 2.5 | −2.02 | 1.07E + 09 | 0.006 |
| 3° − 41 | 243.088 | 243.092 | 17,410 | 2.5 | 428,777 | 3.5 | −2.11 | 8.72E + 08 | 0.007 |
| 3° − 40 | 243.426 | 243.424 | 17,410 | 2.5 | 428,216 | 3.5 | −1.54 | 3.23E + 09 | 0.012 |
| 3° − 39 | 243.434 | 243.434 | 17,410 | 2.5 | 428,199 | 1.5 | −1.51 | 3.45E + 09 | 0.121 |
| 1° − 26 | 243.518 | 243.514 | 0 | 3.5 | 410,654 | 3.5 | −2.01 | 1.11E + 09 | 0.004 |
| 2° − 27 | 243.551 | 243.554 | 1233 | 1.5 | 411,819 | 2.5 | −1.96 | 1.23E + 09 | 0.073 |
| 1° − 24 | | 244.095 | 0 | 3.5 | 409,676 | 2.5 | −3.96 | 1.24E + 07 | 0.000 |
| 4° − 69 | | 244.249 | 89,123 | 0.5 | 498,541 | 1.5 | 0.08 | 1.33E + 11 | 0.183 |
| 1° − 23 | 244.281 | 244.283 | 0 | 3.5 | 409,362 | 2.5 | −1.30 | 5.53E + 09 | 0.088 |
| 2° − 25 | | 244.484 | 1233 | 1.5 | 410,258 | 1.5 | −2.54 | 3.21E + 08 | 0.005 |
| 2° − 24 | 244.833 | 244.832 | 1233 | 1.5 | 409,676 | 2.5 | −1.36 | 4.86E + 09 | 0.473 |
| 3° − 38 | 244.839 | 244.838 | 17,410 | 2.5 | 425,843 | 1.5 | −1.19 | 7.21E + 09 | 0.142 |
| 1° − 21 | 245.046 | 245.046 | 0 | 3.5 | 408,086 | 3.5 | −0.81 | 1.71E + 10 | 0.041 |
| 2° − 22 | 245.334 | 245.339 | 1233 | 1.5 | 408,833 | 1.5 | −2.00 | 1.11E + 09 | 0.079 |
| 3° − 37 | 245.474 | 245.476 | 17,410 | 2.5 | 424,781 | 2.5 | −1.26 | 6.09E + 09 | 0.060 |
| 1° − 20 | 246.362 | 246.362 | 0 | 3.5 | 405,907 | 4.5 | −0.73 | 2.06E + 10 | 0.359 |
| 4° − 66 | 248.007 | 248.007 | 89,123 | 0.5 | 492,337 | 0.5 | −1.01 | 1.07E + 10 | 0.016 |
| 3° − 36 | 248.508 | 248.508 | 17,410 | 2.5 | 419,811 | 2.5 | −0.71 | 2.11E + 10 | 0.080 |
| 3° − 35 | 248.649 | 248.648 | 17,410 | 2.5 | 419,585 | 3.5 | −0.61 | 2.65E + 10 | 0.130 |
| 1° − 19 | 248.765 | 248.766 | 0 | 3.5 | 401,984 | 2.5 | −0.37 | 4.61E + 10 | 0.069 |
| 2° − 19 | 249.533 | 249.532 | 1233 | 1.5 | 401,984 | 2.5 | 0.03 | 1.16E + 11 | 0.551 |

**Table 3.** *Cont.*

| Indexes [a] | Wavelength [b] | | Lower Odd Level [c] | | Upper Even Level [c] | | | | |
|---|---|---|---|---|---|---|---|---|---|
| | $\lambda_{exp}$ (Å) | $\lambda_{Ritz}$ (Å) | E ($cm^{-1}$) | J | E ($cm^{-1}$) | J | log gf [d] | gA ($s^{-1}$) [d] | CF [e] |
| 1° − 18 | 249.873 | 249.873 | 0 | 3.5 | 400,203 | 4.5 | −0.65 | 2.39E + 10 | 0.152 |
| 3° − 33 | 250.010 | 250.010 | 17,410 | 2.5 | 417,394 | 1.5 | −1.13 | 7.92E + 09 | 0.141 |
| 4° − 65 | | 250.766 | 89,123 | 0.5 | 487,901 | 1.5 | −2.70 | 2.11E + 08 | 0.002 |
| 1° − 17 | 250.811 | 250.811 | 0 | 3.5 | 398,707 | 4.5 | −1.06 | 9.19E + 09 | 0.031 |
| 3° − 31 | 250.978 | 250.978 | 17,410 | 2.5 | 415,852 | 2.5 | −1.01 | 1.03E + 10 | 0.057 |
| 1° − 16 | 251.500 | 251.501 | 0 | 3.5 | 397,612 | 2.5 | −1.25 | 5.87E + 09 | 0.041 |
| 3° − 30 | 251.584 | 251.586 | 17,410 | 2.5 | 414,888 | 3.5 | −0.43 | 3.94E + 10 | 0.150 |
| 1° − 14 | 252.203 | 252.204 | 0 | 3.5 | 396,505 | 3.5 | −0.34 | 4.82E + 10 | 0.116 |
| 2° − 16 | 252.285 | 252.284 | 1233 | 1.5 | 397,612 | 2.5 | −1.05 | 9.30E + 09 | 0.413 |
| 2° − 15 | 252.740 | 252.742 | 1233 | 1.5 | 396,894 | 1.5 | 0.08 | 1.27E + 11 | 0.330 |
| 1° − 12 | 252.862 | 252.863 | 0 | 3.5 | 395,471 | 3.5 | −1.54 | 3.04E + 09 | 0.001 |
| 1° − 11 | 252.989 | 252.988 | 0 | 3.5 | 395,276 | 2.5 | −1.50 | 3.31E + 09 | 0.027 |
| 3° − 28 | 253.534 | 253.536 | 17,410 | 2.5 | 411,832 | 3.5 | −0.92 | 1.23E + 10 | 0.110 |
| 3° − 27 | 253.541 | 253.544 | 17,410 | 2.5 | 411,819 | 2.5 | −0.04 | 9.56E + 10 | 0.131 |
| 2° − 13 | 253.653 | 253.652 | 1233 | 1.5 | 395,474 | 0.5 | −0.44 | 3.73E + 10 | 0.140 |
| 4° − 63 | 253.726 | 253.730 | 89,123 | 0.5 | 483,243 | 1.5 | −1.49 | 3.35E + 09 | 0.013 |
| 2° − 11 | 253.779 | 253.779 | 1233 | 1.5 | 395,276 | 2.5 | −2.40 | 4.08E + 08 | 0.024 |
| 1° − 10 | 253.812 | 253.812 | 0 | 3.5 | 393,992 | 3.5 | 0.09 | 1.26E + 11 | 0.101 |
| 3° − 26 | 254.294 | 254.295 | 17,410 | 2.5 | 410,654 | 3.5 | 0.01 | 1.04E + 11 | 0.143 |
| 3° − 25 | 254.551 | 254.551 | 17,410 | 2.5 | 410,258 | 1.5 | −0.02 | 9.92E + 10 | 0.190 |
| 3° − 24 | 254.928 | 254.929 | 17,410 | 2.5 | 409,676 | 2.5 | −0.92 | 1.23E + 10 | 0.039 |
| 3° − 23 | 255.140 | 255.133 | 17,410 | 2.5 | 409,362 | 2.5 | −2.03 | 9.57E + 08 | 0.013 |
| 1° − 9 | 255.401 | 255.401 | 0 | 3.5 | 391,541 | 4.5 | 0.32 | 2.16E + 11 | 0.165 |
| 3° − 22 | 255.479 | 255.478 | 17,410 | 2.5 | 408,833 | 1.5 | −0.99 | 1.05E + 10 | 0.076 |
| 3° − 21 | 255.967 | 255.967 | 17,410 | 2.5 | 408,086 | 3.5 | −0.40 | 4.09E + 10 | 0.115 |
| 1° − 8 | 258.592 | 258.596 | 0 | 3.5 | 386,704 | 2.5 | 0.05 | 1.10E + 11 | 0.210 |
| 4° − 60 | 259.069 | 259.071 | 89,123 | 0.5 | 475,117 | 1.5 | −0.86 | 1.39E + 10 | 0.048 |
| 2° − 8 | 259.419 | 259.423 | 1233 | 1.5 | 386,704 | 2.5 | −0.24 | 5.66E + 10 | 0.293 |
| 3° − 19 | 260.027 | 260.028 | 17,410 | 2.5 | 401,984 | 2.5 | −1.63 | 2.29E + 09 | 0.015 |
| 1° − 7 | 260.146 | 260.146 | 0 | 3.5 | 384,400 | 4.5 | −1.54 | 2.85E + 09 | 0.009 |
| 1° − 6 | 261.002 | 261.006 | 0 | 3.5 | 383,133 | 2.5 | −1.45 | 3.49E + 09 | 0.029 |
| 1° − 5 | 261.767 | 261.767 | 0 | 3.5 | 382,019 | 3.5 | −0.93 | 1.14E + 10 | 0.027 |
| 2° − 6 | 261.849 | 261.849 | 1233 | 1.5 | 383,133 | 2.5 | −2.18 | 6.41E + 08 | 0.004 |
| 1° − 4 | 262.537 | 262.537 | 0 | 3.5 | 380,899 | 4.5 | −1.28 | 5.12E + 09 | 0.005 |
| 3° − 16 | | 263.018 | 17,410 | 2.5 | 397,612 | 2.5 | −2.22 | 5.79E + 08 | 0.004 |
| 3° − 15 | 263.521 | 263.516 | 17,410 | 2.5 | 396,894 | 1.5 | −2.89 | 1.24E + 08 | 0.001 |
| 3° − 14 | 263.787 | 263.786 | 17,410 | 2.5 | 396,505 | 3.5 | −1.41 | 3.74E + 09 | 0.014 |
| 3° − 12 | 264.508 | 264.508 | 17,410 | 2.5 | 395,471 | 3.5 | −1.04 | 8.63E + 09 | 0.014 |
| 1° − 3 | 264.644 | 264.643 | 0 | 3.5 | 377,867 | 2.5 | −1.07 | 8.00E + 09 | 0.032 |
| 3° − 11 | 264.644 | 264.644 | 17,410 | 2.5 | 395,276 | 2.5 | −1.22 | 5.67E + 09 | 0.016 |
| 1° − 1 | 265.168 | 265.168 | 0 | 3.5 | 377,119 | 4.5 | −1.02 | 8.91E + 09 | 0.013 |
| 2° − 3 | 265.510 | 265.510 | 1233 | 1.5 | 377,867 | 2.5 | −1.26 | 5.18E + 09 | 0.031 |

**Table 3.** *Cont.*

| Indexes [a] | Wavelength [b] | | Lower Odd Level [c] | | Upper Even Level [c] | | | | |
|---|---|---|---|---|---|---|---|---|---|
| | $\lambda_{exp}$ (Å) | $\lambda_{Ritz}$ (Å) | E ($cm^{-1}$) | J | E ($cm^{-1}$) | J | log gf [d] | gA ($s^{-1}$) [d] | CF [e] |
| 2° − 2 | 265.919 | 265.919 | 1233 | 1.5 | 377,288 | 1.5 | −1.47 | 3.16E + 09 | 0.055 |
| 4° − 56 | 267.518 | 267.520 | 89,123 | 0.5 | 462,927 | 1.5 | −2.82 | 1.42E + 08 | 0.002 |
| 3° − 8 | 270.794 | 270.787 | 17,410 | 2.5 | 386,704 | 2.5 | −2.53 | 2.66E + 08 | 0.001 |
| 4° − 54 | 270.816 | 270.814 | 89,123 | 0.5 | 458,380 | 1.5 | −1.34 | 4.11E + 09 | 0.019 |
| 3° − 5 | | 274.266 | 17,410 | 2.5 | 382,019 | 3.5 | −2.84 | 1.28E + 08 | 0.000 |
| 4° − 50 | | 274.953 | 89,123 | 0.5 | 452,821 | 1.5 | −1.07 | 7.47E + 09 | 0.022 |
| 3° − 3 | | 277.426 | 17,410 | 2.5 | 377,867 | 2.5 | −1.92 | 1.03E + 09 | 0.004 |
| 4° − 39 | | 294.919 | 89,123 | 0.5 | 428,199 | 1.5 | −3.08 | 6.41E + 07 | 0.003 |
| 4° − 38 | | 296.983 | 89,123 | 0.5 | 425,843 | 1.5 | −2.64 | 1.75E + 08 | 0.029 |
| 4° − 33 | | 304.626 | 89,123 | 0.5 | 417,394 | 1.5 | −2.92 | 8.72E + 07 | 0.008 |
| 4° − 25 | | 311.396 | 89,123 | 0.5 | 410,258 | 1.5 | −2.23 | 4.06E + 08 | 0.008 |
| 4° − 22 | | 312.783 | 89,123 | 0.5 | 408,833 | 1.5 | −3.21 | 4.21E + 07 | 0.004 |
| 4° − 15 | | 324.917 | 89,123 | 0.5 | 396,894 | 1.5 | −2.78 | 1.04E + 08 | 0.000 |
| 4° − 13 | | 326.423 | 89,123 | 0.5 | 395,474 | 0.5 | −2.44 | 2.28E + 08 | 0.002 |
| 4° − 2 | | 347.023 | 89,123 | 0.5 | 377,288 | 1.5 | −3.14 | 3.94E + 07 | 0.002 |

[a] Indexes of levels as given in Table 2. [b] $\lambda_{exp}$ are taken from [13] while $\lambda_{Ritz}$ are deduced from experimental energy levels given by the same authors. [c] From [13]. [d] This work : model HFR(F). [e] Cancellation factor as defined in Equation (6).

On the other hand, one spectral line observed at 198.625 Å by Ryabtsev *et al.* [13] is not present in Table 3. This can be explained by the fact that, for this transition, our calculated oscillator strength is unexpectedly found to be much smaller than the cut-off chosen for drawing up the table (log $gf > -4$). The reason could be found in the strong cancellation effects affecting the calculation of the line strength corresponding to this transition for which our HFR values are log $gf = -4.44$ and $gA = 6.16\text{E} + 06$ $s^{-1}$. As a reminder, in order to calculate $gA$ or $gf$ for a transition between the atomic states $\gamma J$ and $\gamma' J'$, we have to compute the value of the line strength

$$S = \left| \left\langle \gamma J \left\| P^{(1)} \right\| \gamma' J' \right\rangle \right|^2 \tag{1}$$

or that of its square root

$$S^{1/2} = \left\langle \gamma J \left\| P^{(1)} \right\| \gamma' J' \right\rangle \tag{2}$$

where $P^{(1)}$ is the electric dipole operator. Because of intermediate coupling and configuration interaction mixing, the wavefunctions are expanded in terms of basis functions:

$$\left| \gamma J \right\rangle = \sum_{\beta} y_{\beta J}^{\gamma} \left| \beta J \right\rangle \tag{3}$$

$$\left| \gamma' J' \right\rangle = \sum_{\beta'} y_{\beta' J'}^{\gamma'} \left| \beta' J' \right\rangle \tag{4}$$

We may then write Equation (2) in the form

$$S^{1/2} = \sum_{\beta} \sum_{\beta'} y_{\beta J}^{\gamma} \left\langle \beta J \left\| P^{(1)} \right\| \beta' J' \right\rangle y_{\beta' J'}^{\gamma'} \tag{5}$$

This sum thus represents a mixing of amplitudes rather than line strengths themselves with the consequence that the effect of mixing is not necessarily a tendency to average out the various line strengths. There are frequently destructive interference effects that cause a weak line to become still weaker. In this context, the cancellation factor is given by

$$CF = \left[ \frac{\left| \sum_{\beta} \sum_{\beta'} y^{\gamma}_{\beta J} \left\langle \beta J \left\| P^{(1)} \right\| \beta' J' \right\rangle y^{\gamma'}_{\beta' J'} \right|}{\sum_{\beta} \sum_{\beta'} \left| y^{\gamma}_{\beta J} \left\langle \beta J \left\| P^{(1)} \right\| \beta' J' \right\rangle y^{\gamma'}_{\beta' J'} \right|} \right]^2 \quad (6)$$

According to Cowan [18], very small values of this factor (typically when *CF* is smaller than about 0.02) indicate that the corresponding transition rates may be expected to show large percentage errors. In Table 3, *CF*-factors are given for each line in order to give an idea of the reliability of the corresponding transition rates. It is clear that many lines with computed *gA*-values smaller than $10^9$ $s^{-1}$ are affected by very small values of *CF* indicating that the corresponding transition rates must be taken with caution. On the contrary, most of the strongest transitions listed in Table 3, in particular those with $gA > 10^{10}$ $s^{-1}$, do not appear to be affected by cancellation effects.

Finally, in Figure 3, we compare our transition probabilities with those reported by Ryabtsev *et al.* [13]. As expected, a rather large scatter is observed between both sets of results. However, as already discussed in Section 3, in view of the much more extended configuration interaction model adopted here in comparison with the rather limited physical model used by Ryabtsev *et al.*, in particular in the odd parity, the decay rates obtained in the present work should indisputably be more accurate.

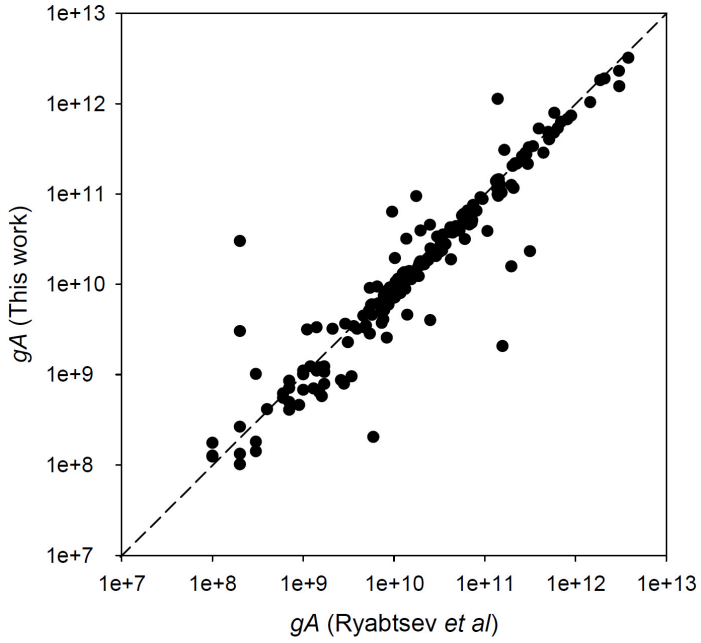


**Figure 3.** Comparison between the transition probabilities (*gA* in $s^{-1}$) computed in the present work and those obtained by Ryabtsev *et al.* [13] for experimentally identified spectral lines in W VIII.

For plasma diagnostic purposes, it is sometimes useful to know the decay rates corresponding to forbidden lines. In the present work, such parameters were thus also computed for magnetic dipole

(M1) and electric quadrupole (E2) transitions involving the four experimentally known levels within the odd parity of W VIII. It was found that only three transitions could be considered as having rather strong transition probabilities. These lines are the following: (1) $\lambda_{vac}$ = 1137.79 Å, $E_{low}$ = 1233 cm$^{-1}$ ($J$ = 3/2) − $E_{up}$ = 89,123 cm$^{-1}$ ($J$=1/2), $gA$(M1 + E2) = 2.55 × 10$^4$ s$^{-1}$, (2) $\lambda_{vac}$ = 1394.45 Å, $E_{low}$ = 17,410 cm$^{-1}$ ($J$ = 5/2) − $E_{up}$ = 89,123 cm$^{-1}$ ($J$=1/2), $gA$(E2) = 6.54 × 10$^1$ s$^{-1}$, and (3) $\lambda_{air}$ = 5742.26 Å, $E_{low}$ = 0 cm$^{-1}$ ($J$ = 7/2) − $E_{up}$ = 17,410 cm$^{-1}$ ($J$=5/2), $gA$(M1) = 4.90 × 10$^2$ s$^{-1}$.

## 5. Conclusions

A detailed analysis of configuration interaction effects in seven times ionized tungsten allowed us to give a new reliable set of transition probabilities and oscillator strengths for lines of this ion in the spectral range from 160 to 347 Å. The final results were obtained within the framework of an extended physical model based on the pseudo-relativistic Hartree-Fock approach combined with a semi-empirical optimization of the radial energy parameters. Just like our previous studies related to the lowest ionization stages of W, it is expected that the radiative data reported in the present work for the W VIII spectrum will be useful for plasma diagnostics in future fusion reactors where tungsten will be used as a plasma facing material.

## Acknowledgments

Pascal Quinet is Research Director of the Belgian National Fund for Scientific Research F.R.S.-FNRS. Financial support from this organization is acknowledged.

## Author Contributions

Both authors were equally involved in the calculations reported in the present paper as well as in the the writing of the manuscript.

## Conflicts of Interest

The authors declare no conflict of interest.

## References

1. Federici, G.; Skinner, C.H.; Brooks, J.N.; Coad, J.P.; Grisolia, C.; Haasz, A.A.; Hassanein, A.; Philipps,V.; Pitcher, C.S.; Roth, J.; *et al.* Plasma-material interactions in current tokamaks and their implications for next step fusion reactors. *Nucl. Fusion* **2001**, *41*, 1967–2138.
2. Neu, R.; Dux, R.; Kallenbach, A.; Pütterich, T.; Balden, M.; Fuchs, J.C.; Herrmann, A.; Maggi, C.F.; O'Mullane, M.; Pugno, R.; *et al.* Tungsten: An option for divertor and main chamber plasma facing components in future fusion devices. *Nucl. Fusion* **2005**, *45*, 209–218.
3. Pospieszczyk, A. *Nuclear Fusion Research*; Springer: Berlin, Germany, 2006.
4. Skinner, C.H. Applications of EBIT to magnetic fusion diagnostics. *Can. J. Phys*. **2008**, *86*, 285–290.
5. Skinner, C.H. Atomic physics in the quest for fusion energy and ITER. *Phys. Scr*. **2009**, *T134*, 014022.

6. Quinet, P.; Palmeri, P.; Biémont, E. Spectroscopic data for atomic tungsten transitions of interest in fusion plasma research. *J. Phys. B At. Mol. Opt. Phys*. **2011**, *44*, 145005.
7. Nilsson, H.; Engström, L.; Lundberg, H.; Palmeri, P.; Fivet, V.; Quinet, P.; Biémont, E. Lifetime measurements and transition probability calculations in singly ionized tungsten (W II). *Eur. Phys. J. D* **2008**, *49*, 13–19.
8. Palmeri, P.; Quinet, P.; Fivet, V.; Biémont, E.; Nilsson, H.; Engström, L.; Lundberg, H. Lifetime measurements and calculated transition probabilities in W III. *Phys. Scr*. **2008**, *78*, 015304.
9. Enzonga Yoca, S.; Quinet, P.; Biémont, E. Configuration interaction and radiative decay rates in trebly ionized tungsten (W IV). *J. Phys. B At. Mol. Opt. Phys.* **2012**, *45*, 035001.
10. Enzonga Yoca, S.; Quinet, P.; Palmeri, P.; Biémont, E. Comparative semi-empirical and *ab initio* atomic structure calculations in Yb-like tungsten $W^{4+}$. *J. Phys. B Mol. Opt. Phys*. **2012**, *45*, 065001.
11. Enzonga Yoca, S.; Palmeri, P.; Quinet, P.; Jumet, G.; Biémont, E. Radiative properties and core-polarization effects in the $W^{5+}$ ion. *J. Phys. B At. Mol. Opt. Phys*. **2012**, *45*, 035002.
12. Quinet, P.; Vinogradoff, V.; Palmeri, P.; Biémont, E. Radiative decay rates for W I, W II and W III allowed and forbidden transitions of interest for spectroscopic diagnostics in fusion plasmas. *J. Phys. B At. Mol. Opt. Phys*. **2010**, *43*, 144003.
13. Ryabtsev, A.N.; Kononov, E.Y.; Kildiyarova, R.R.; Tchang-Brillet, W.-Ü.L.; Wyart, J.-F. The spectrum of seven times ionized tungsten (W VIII) relevant to tokamak divertor plasmas. *Phys. Scr*. **2013**, *87*, 045303.
14. Kramida, A.E.; Shirai, T. Energy levels and spectral lines of tungsten, W III through W LXXIV. *At. Data Nucl. Data Tables* **2009**, *95*, 305–474.
15. Sugar, J.; Kaufman, V. Seventh spectrum of tungsten (W VII); resonance lines of Hf V. *Phys. Rev. A* **1975**, *12*, 994–1012.
16. Carlson, T.A.; Nestor, C.W.Jr.; Wasserman, N.; McDowell, J.D. Calculated ionization potentials for multiply charged ions. *At. Data Nucl. Data Tables* **1970**, *2*, 63–99.
17. Veres, G.; Bakos, J.S.; Kardon, B. Energy levels and the vacuum ultraviolet spectrum of W VIII. *J. Quant. Spectrosc. Rad. Transfer* **1996**, *56*, 295–301.
18. Cowan, R.D. *The Theory of Atomic Structure and Spectra*; University of California Press: Berkeley, CA, USA, 1981.
19. Quinet, P.; Hansen, J.E. The influence of core excitations on energies and oscillator strengths of iron group elements. *J. Phys. B At. Mol. Opt. Phys*. **1995**, *28*, L213–L220.